DESIGN OPTIMIZATION AND EFFICIENCY MODELING OF A HOT GAS VANE MOTOR

A thesis presented to the faculty of the Graduate School
University of Missouri-Columbia

In Partial Fulfillment
Of the Requirements for the Degree
Master of Science

By

GREGORY BOMMARITO

Dr. Roger Fales, Thesis Supervisor

December 2007

The undersigned, appointed by the dean of the Graduate School, have examined the project entitled

DESIGN OPTIMIZATION AND EFFICIENCY MODELING OF A HOT GAS VANE MOTOR

Presented by Gregory Bommarito

a candidate for the degree of Masters of Science

and hereby certify that in their opinion it is worthy of acceptance.

Dr. Roger Fales, Assistant Professor, Mechanical and Aerospace Engineering

---

Dr. Craig Kluever, Professor, Mechanical and Aerospace Engineering

---

Dr. Steven Borgelt, Associate Professor, Agricultural Systems Management

ACKNOWLEDGEMENTS

Most of all I would like to thank my mentor Dr. Roger Fales for all the support he provided me throughout this project. His motivation and passion for engineering were a constant source of inspiration both on this project and in the classroom. I am very grateful for the many hours of instruction that I have received from Dr. Fales. I only hope that some day I may achieve as complete of an understanding of engineering systems as he has.

I would like to thank the members of Vanderbilt University who collaborated on this work with me, especially Dr. Eric Barth, Dr. Michael Goldfarb, Bo Li, and Jason Mitchell whose support was indispensable. Their ideas helped guide me throughout this project.

I would like to thank Dr. Craig Kluever for improving my education in both my undergraduate and graduate courses. I admire the passion he has for his work in education and am honored that I had the privilege of being his student.

I would like to thank Dr. Steven Borgelt for assisting in the improvement of this work and for participating in my thesis committee.

I would like to thank my friend and colleague Adam Molitor, who was always willing to lend a helping hand or a sympathetic ear.

Finally, I would like to thank my parents, Sam and Bonnie Bommarito, for their support throughout my college career. They have allowed me to achieve my dreams, and I only hope that I can some day repay them for all that they have done for me.

TABLE OF CONTENTS

LIST OF FIGURES

LIST OF TABLES

NOMENCLATURE

Symbol	Description	Units
a	Acceleration	m/s^2
A_a	Exposed area of the aft vane	m^2
$A_{ex,i}$	Exhaust area	m^2
A_f	Exposed area of the fore vane	m^2
A_v	Area of vane tip	m^2
$A_{v,in}$	Area of the injection valve	m^2
b_{load}	Viscous rotational damping	kgm^2/s
C_f	Valve discharge coefficient	-
c_p	Specific heat at constant pressure	J/kg/K
C_r	Pressure ratio at which flow becomes choked	-
e	Offset distance between rotor and stator centers	m
E	Energy	J
F_f	Friction force	N
F_{na}	Normal force due to acceleration of vane	N
F_{np}	Normal force including pressure forces	N
J_{load}	Rotational inertia	kgm^2
k	Lower heating value of the hot gas	J/kg
L	Vane length	m
l	Distance from rotor center to edge of stator	m
$\dot{\vec{l}}_r$	Relative velocity of a vane	m/s
$\ddot{\vec{l}}_r$	Relative acceleration of a vane	m/s^2
m	Mass of rotor	kg
$\dot{m}_{in,i}$	Mass flowrate into the *i*th chamber	kg/s
$\dot{m}_{out,i}$	Mass flowrate out of the *i*th chamber	kg/s
Ma	Mach number	-
m_v	Mass of a vane	kg
n	Number of vanes	-
N'	Load per unit width	N/m
P_{atm}	Atmospheric pressure	Pa
P_i	Pressure in the *i*th chamber	Pa
P_s	Supply Pressure	Pa
R	Gas constant	J/kg/K
$\ddot{\vec{R}}$	Absolute acceleration of the coordinate frame	m/s^2
r_a	Moment arm of the aft vane	m
r_f	Moment arm of the fore vane	m
R_R	Radius of the rotor	m
R_S	Radius of the stator	m
t	Vane thickness	m
T_1	Temperature at the inlet	K
T_f	Friction torque	Nm

T_i	Temperature in the *i*th chamber	K
T_s	Total shaft torque	Nm
v	Velocity of the fluid	m/s
V_i	Volume in the *i*th chamber	m^3
W	Vane width	m
W_f	Energy dissipated due to friction	J
α	Stribeck curve coefficient	-
β	Angle between normal direction and vane direction	rad.
γ	Ratio of specific heats	-
ε	Stribeck curve coefficient	-
η	Efficiency	-
η_f	Absolute fluid viscosity	Pa s
θ	Vane position	rad.
μ	Coefficient of friction	-
μ'	Boundary lubrication coefficient	-
ρ_l	Density of liquid propellant	kg/m^3
τ_c	Time Constant	s
$\bar{\omega}$	Angular Velocity	rad./s
$\dot{\bar{\omega}}$	Angular acceleration of the rotor	$rad./s^2$

Abstract

The purpose of this research is to model and analyze the dynamics of a hot gas vane motor for design optimization work. The pneumatic motor is a portable direct drive actuator that is intended as an alternative to battery-powered electromagnetic motors. It is believed that the vane motor could replace other solutions for portable power generation. An optimal design of the motor is desirable to maximize portability and efficiency. Modeling the device will make it possible to optimize the mechanical efficiency by altering the geometry of the motor's vanes and respective chambers. The modeling of the device focuses on determining the net amount of torque that is produced by the high pressures that drive the device. While the efficiency of the motor is affected to a great extent by its geometry, losses from friction will also be considered. A model of Stribeck friction was developed to account for losses from friction. For the device to remain portable, there are limitations on the size of the final design which will restrict the optimal efficiency of the vane motor.

Chapter 1

INTRODUCTION

The purpose of this research is to analyze a unique application of a hot gas vane motor to determine if it is a viable candidate to replace currently used technology. The two most commonly used portable drive devices are battery-powered electric motors and hydrocarbon-fueled internal-combustion-engines. Battery-powered motors offer the advantage of start/stop, quiet operation, but have the disadvantage of low mass-specific power and energy densities. Hydocarbon-fueled combustion engines have superior mass-specific power and energy densities, but do not allow start/stop or bidirectional operation. It is believed that a hot gas vane motor should produce high mass-specific power and energy densities and also should provide quiet, start/stop, bidirectional operation.

The vane motor is not a recent discovery. There is evidence of vane motors from as early as 1868 and there are U.S. patents from 1924 [1]. Early vane motors were typically hydraulic devices, whereas the vane motor under discussion is a pneumatic device. Vane motors for pneumatic systems operate at free speeds up to 13,000 rpm, with rated speed approximately 50% of that level [2]. Vane motors can come in a variety of sizes and styles. The vane motor being discussed in this research is relatively small (< 1 kg in weight), but there are much larger versions of vane motors. For example, the Wankel engine works in a similar fashion to a vane motor and is used in the Mazda RX-8.

The vane motor in this work uses a monopropellant, hydrogen peroxide, as a

power source. Hydrogen peroxide has been used as a monopropellant for many other applications. The Royal Aircraft Establishment of Great Britain used hydrogen peroxide to successfully launch low cost rockets into space, including the Black Knight and Black Arrow rockets. The German military used hydrogen peroxide as a monopropellant in WWII to drive a turbine that powered submarines. Also hydrogen peroxide was used to propel torpedoes from those submarines [3].

1.1 Established Research

Vane motors have been in operation in the United States for nearly a century, and not surprisingly, much research has already been developed. However, as of yet, there has been a limited amount of research aimed at optimizing the efficiency of the device based on geometry. The ultimate goal of this research is to improve the efficiency of a hot gas vane motor through variations in the geometry of the motor. In order to accomplish this task, a viable model of the device needs to be developed. The model constructed for this work is based primarily on the work of Barth, Fite, Goldfarb and Li [1]. Their model of the hot gas vane motor is based on a basic torque equation, which is derived from the relationship between the pressure in each chamber of the device and the geometry of the device at any instant. Pressures are solved for using the first law of thermodynamics and assuming that the ideal gas entering the system undergoes an adiabatic process. The model for this work uses the same assumptions from [1], however, several important features have been added to the model in order to increase the accuracy.

The most important feature added to the system is a model for the frictional

torques that develop during operation. Equating the friction within any system is typically a difficult process, due to the fact that the friction coefficient, μ, is generally unknown and also changes throughout operation. The friction coefficient may be solved for using experimental methods, but analytical methods for solving the friction coefficient have also been developed. One method for approximating the friction coefficient is to use a Stribeck Curve. The dynamic behavior of the coefficient of friction for sliding surfaces has historically been considered using the Stribeck Curve. Research from Manring [4], has shown that a Stribeck friction curve is a good approximation for friction in devices similar to that of a hot gas vane motor.

The friction coefficient is not the only quantity needed to determine the friction torques within the system. The normal forces between the moving surfaces of the hot gas vane motor also need to be known. Research has been done to develop an appropriate free body diagram of the forces within the motor. A detailed diagram of the forces within the system was produced by Bertetto, Mazza, Pastorelli, and Raparelli [5]. Their research showed that the forces on pneumatic motor vanes vary according to the orientation of the vanes relative to the stator or housing of the device. Vanes within the motor have a certain amount of flexibility within the motor, which has an affect on the forces present on those vanes. Their model, however, did not give an in depth description of how to solve for the pressures on the back and tip of the vane.

Research from Inaguma and Hibi [6] shows an appropriate method for solving for pressure forces on the vanes that are present throughout the operation. While their work was for a hydraulic pump, the methodology used is completely relevant for a

hot gas vane motor. Much like the work from Bertetto [5], their work showed that the orientation of the vane and the tip geometry play an important role in defining the forces present on the vanes.

1.2 Research Objectives

The objectives of this research are to develop a detailed model of the hot gas vane motor, and then use that model to optimize the design of the device. Models for hot gas vane motors have been developed, but each model is partially incomplete. In this research, a more complete model of the hot gas vane motor was developed, by expanding on the ideas presented in existing research. Specifically, a more detailed model of friction was developed in order to create a more viable model. The completed model was used to optimize the design and performance of the hot gas vane motor.

1.3 Thesis Outline

Chapter 2 focuses on establishing a basic model for the hot gas vane motor. The research of Michael Goldfarb and Eric Barth, that is being developed at Vanderbilt University serves as the starting point for the model development. Their research is the fundamental basis for the model and this research. Chapter 3 works to expand the model and increase its precision. This is accomplished by developing a more accurate friction model, using more detailed dynamics. In addition, it is shown that integrating the Stribeck Curve into the model gives a more accurate approximation of friction within the system. Chapter 4 expands on Chapters 2 and 3,

and shows that a more detailed description of the pressure forces on the vanes is needed in order to give an appropriate description of the friction torque. Chapter 5 shows how the fully developed model may now be used to design a more efficient hot gas vane motor. Finally, overall conclusions and recommendations about future work are presented in Chapter 6.

Chapter 2

Modeling of the Hot Gas Vane Motor

2.1 Basic Operation

A hot gas vane motor is a device that uses hot gas as a power source to drive a shaft and produce power. The motor consists of a circular rotor that is offset in an elliptical stator. Extendable vanes are attached to the rotor and are extended to the inner edge of the stator. During startup, the vanes are held against the stator by a leaf spring. Figure 1 displays a single vane with thickness, *t*, width, *W*, and length, *L*, and the attached leaf spring.

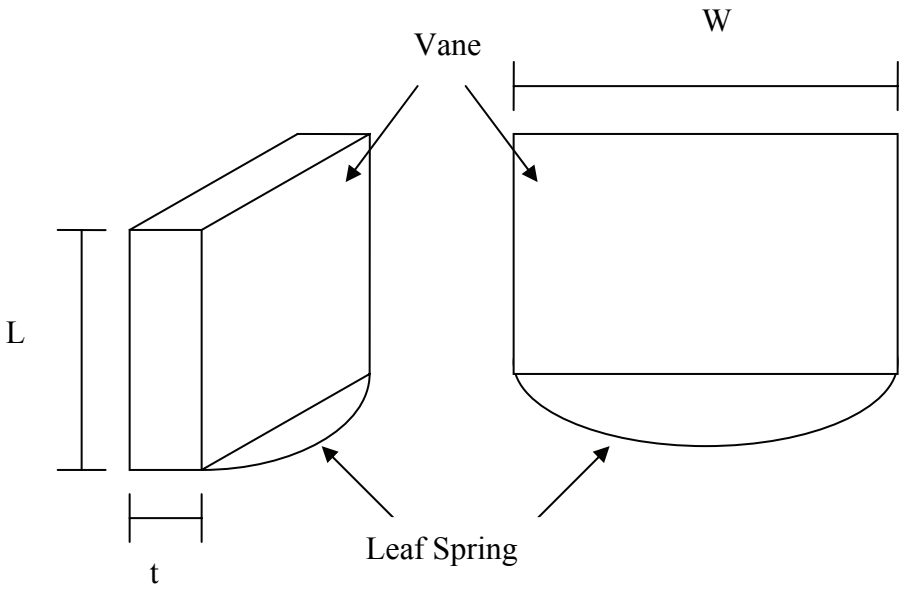

Figure 1. Vane and attached leaf spring.

The leaf spring only provides enough force to keep the vane in contact with the stator at start up. During operation, the vanes are kept in contact with the edge of the stator by the centrifugal force created by the rotor's rotation. There are six vanes

total which create six separate chambers. It is assumed that the thickness of the vanes is negligible so each chamber occupies 1/6th of the total volume of the device. The device is driven by a hot gas that flows into these chambers to create a torque on the shaft attached to the rotor. The vanes are arranged in such a way that the leading vane is always extended further than the trailing vane. Therefore, the pressure from the hot gas causes an increased moment arm on the leading vane, thus creating a net torque. A cross section of the motor is displayed in Figure 2.

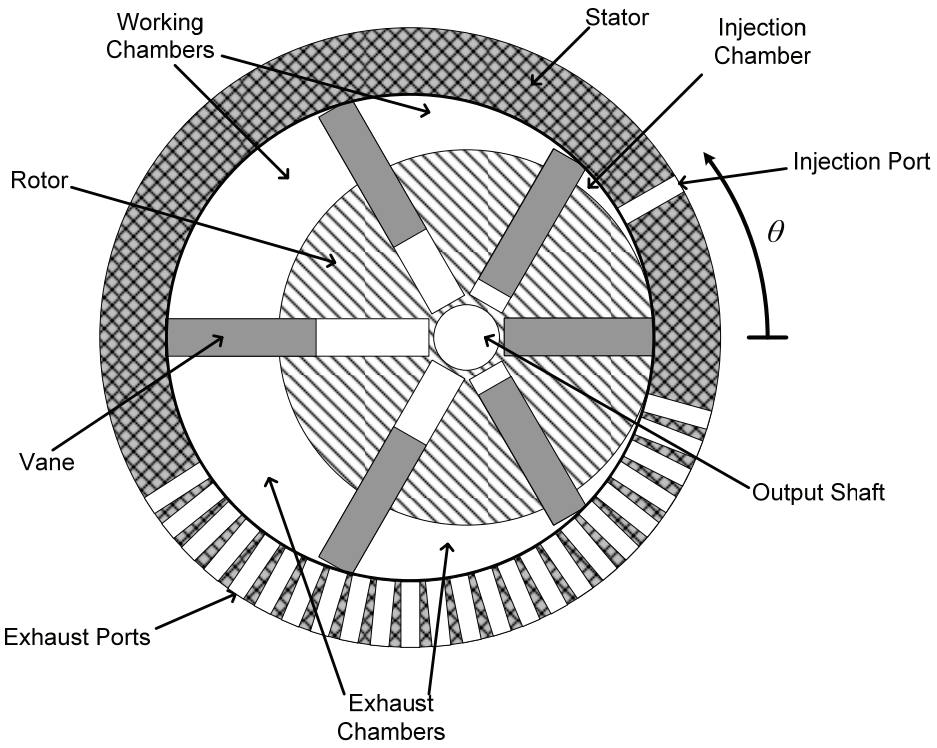

Figure 2. Cross-sectional view of the vane motor.

Exhaust ports are present 210 degrees from the inlet port and continue for an additional 120 degrees. Once the hot gas has rotated through 210 degrees, it is at a much lower pressure and is cooler so it is exhausted into the atmosphere.

The leading vane of a chamber will begin to become extended less than the trailing vane once it has rotated much past 210 degrees. If working fluid were still trapped with no exit ports in the chamber, a negative torque would be created which would adversely affect the performance. All working fluid should be expelled from the motor before it has rotated a full 390 degrees. At this point hot gas is allowed to flow into the working chamber through the injection port and the cycle repeats itself. The hot gas is created by forcing a monopropellant, hydrogen peroxide, to flow through a catalyst pack which causes an exothermic reaction thus creating a stream of high pressure hot gas.

The catalyst pack is typically either a silver or platinum screen that triggers the decomposition. The following equation from [3] shows how the hydrogen peroxide is broken down during the reaction.

$$2H_2O_2 = 2H_2O + O_2 \tag{2.1}$$

Both steam and oxygen are produced in the reaction at about 232 ºC (450 ºF) and this is what drives the device. The hot gas flows into the working chambers through the inlet injection port seen in Figure 2.

2.2 Basic Modeling

The initial modeling of the hot gas vane motor is based off of research that is being completed at Vanderbilt by Barth, Fite, Goldfarb and Li [1]. Specifically, the

equations for torque, pressure, temperature, and mass flowrate are taken from the Vanderbilt research. The model equations are reviewed here. The entire system is driven by torque created because the leading vane in each working chamber has a larger area and a higher pressure than the trailing vane and therefore produces a higher moment arm. The net torque created is defined in Eqn. (2.2) and is simply a function of the pressure in the chamber and the geometry of the motor.

$$T_s(t) = \sum_1^n P_i(t)\left[A_f r_f \theta_f(t) - A_a r_a \theta_a(t) \right]_i \tag{2.2}$$

where T_s is the total shaft torque, N is the total number of chambers in the rotor, P_i is the pressure in the ith chamber, A_f, r_f, and θ_f(t) and A_f, r_f, and θ_f(t) are the exposed vane area, average moment arm, and angle (relative to the stator) of the fore and aft vanes for the ith chamber. Figure 3 displays the areas, moment arms, and pressure of a single chamber.

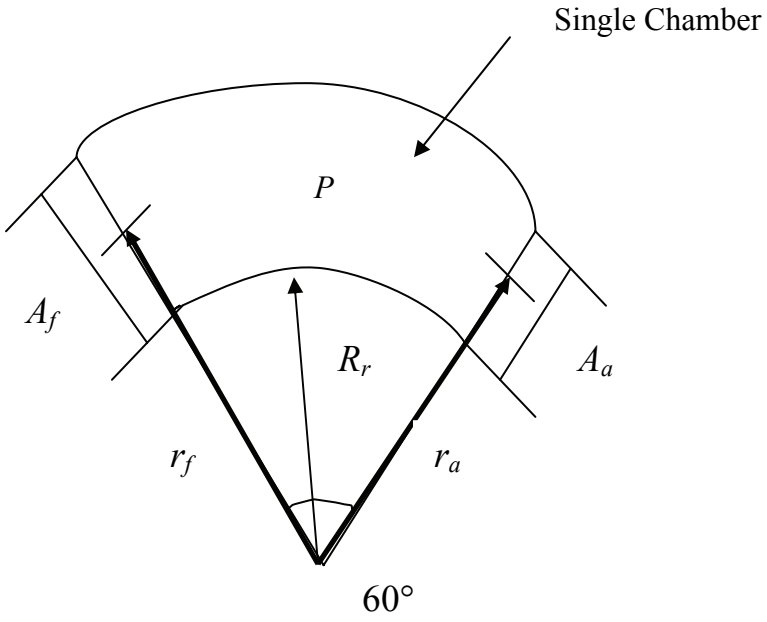

Figure 3. Single chamber of the hot gas vane motor.

The areas and moment arms of each chamber can be determined from the geometry of the motor. Figure 4 displays the orientation of a single vane with length, *l,* on the hot gas vane motor using an **xy** coordinate system.

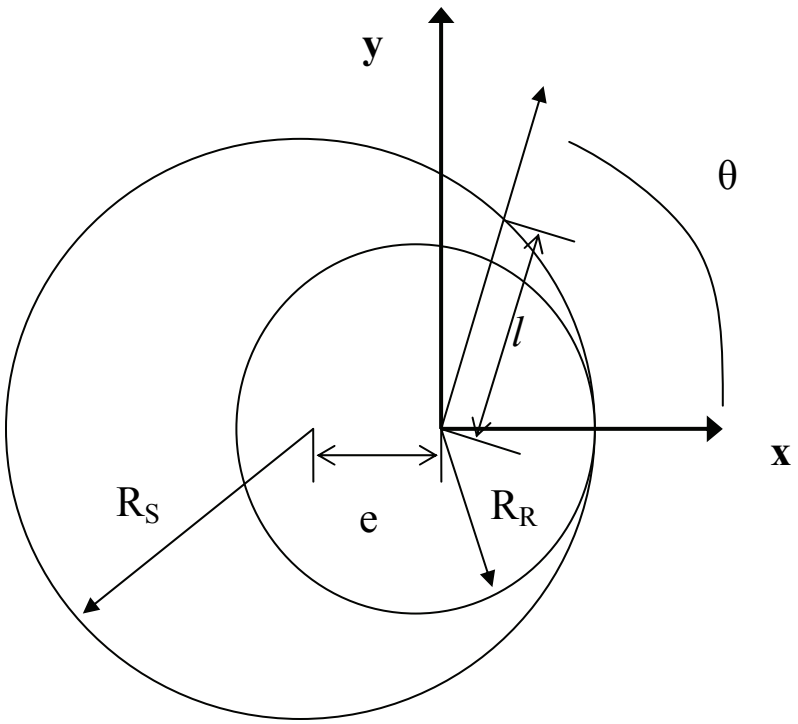

Figure 4. View of a single vane in an **xy** coordinate frame.

From the coordinate system shown in Figure 4, it can be seen that in the **xy** coordinate system

$$x = l\cos(\theta)$$
$$y = l\sin(\theta) \tag{2.3}$$

The equation for the surface of the stator may be defined as follows,

$$(x+e)^2 + y^2 = {R_S}^2 \tag{2.4}$$

where e is the offset distance between the centers of the rotor and stator, and R_S is the radius of the stator. By substituting (2.3) into (2.4) the following quadratic equation can be determined,

$$l^2 + 2e\cos(\theta)l - ({R_S}^2 - e^2) = 0 \tag{2.5}$$

Solving this equation for l yields the following result,

$$l = -e\cos(\theta) + \sqrt{{R_S}^2 - (e\sin(\theta))^2} \tag{2.6}$$

Once the equation for the length of a vane is known, solving for the moment arm, r, is simple. The moment arm is the distance from the center of rotation to the point where the perpendicular force is applied. In this case the force is applied by the pressure from the preceding chamber at the midpoint of the exposed vane. Therefore, the moment arm is defined by the following equation:

$$r = l - \left(\frac{l - R_r}{2}\right) \tag{2.7}$$

where R_r is the radius of the rotor. Solving for the exposed vane area, A, is also possible once the length of the vane is known. The area is defined by the following:

$$A = \left(l - R_r\right)W \tag{2.8}$$

where W is the width of the vane.

Once the pressures in each chamber are known, Eqns. (2.7) and (2.8) may be used with Eqn. (2.2) to solve for the net torque of the system. It is assumed that throughout the entire cycle the hot gas is an ideal gas and that the hot gas remains a gas throughout operation. It is likely that some of the gas may condense to a liquid at

some point which would alter the performance of the device by reducing pressure, but for now it is assumed that the hot gas remains a gas throughout operation. By using the first law of thermodynamics and assuming that the ideal gas undergoes an adiabatic process, the pressure in each chamber can be defined as:

$$\dot{P}_i = \gamma \frac{RT_i}{V_i}\left(\dot{m}_{in,i} - \dot{m}_{out,i}\right) - \gamma \frac{P_i}{V_i}\dot{V}_i \tag{2.9}$$

where $\dot{m}_{in,i}$ and $\dot{m}_{out,i}$ are the inlet and outlet mass flow rates into and out of the *i*th chamber, γ is the ratio of specific heat at constant pressure to specific heat at constant volume, V_i is the volume in the *i*th chamber, and T_i is the temperature in the *i*th chamber.

In this work, integration will be used to find the volume of each chamber. Each chamber occupies a 60 degree section of a circle whose radius is changing according to Eqn. (2.6). Figure 5 shows a triangular shaped differential section of the circle with radius, *l*, at some value of θ.

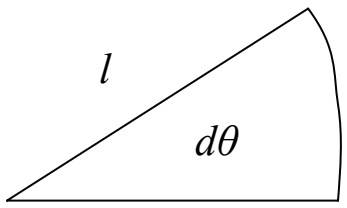

Figure 5. Differential section of a chamber.

The area of this section of circle is approximately equal to a fraction of the total area of a circle with radius, *l*. In other words:

$$dA = \pi l^2 \frac{d\theta}{2\pi} \tag{2.10}$$

In order to solve for the volume of a particular chamber, the area of a 60 degree section is first solved for and then multiplied by the width of the vane motor. However, each section of this circle has 1/6th of the area of the rotor present, which needs to be subtracted off as this is not part of the chamber. In doing so, the volume of a particular chamber may be solved for using the following equation:

$$V = W\left(\int_{\theta-\pi/3}^{\theta} \frac{l^2}{2} d\theta - \frac{\pi R_r^{\,2}}{6}\right) \tag{2.11}$$

Since *l* only depends on θ as seen in Eqn. (2.6), Eqn. (2.11) may be used to solve for the volume in a chamber.

The next unknown in Eqn. (2.9) is the temperature in a chamber. Temperature may be defined by the geometry of the hot gas vane motor. If it is assumed that the process is adiabatic and that the working fluid is an ideal gas, the temperature may be defined by the following:

$$\frac{T_2}{T_1} = \left(\frac{V_1}{V_2}\right)^{\gamma-1} \tag{2.12}$$

where V_2 and T_2 are the volume and temperature in the *i*th chamber respectively and P_1 and T_1 are the initial pressures and temperatures of a working chamber respectively.

Matlab® and Simulink® models were used to integrate the preceding equation and solve for pressure in the *i*th chamber using numerical differential equation solvers. There are six separate chambers so six separate pressures were solved for. Once pressure is known, only the inlet and outlet mass flows need to be

determined to solve for total torque. The mass flow rate into the motor chamber, *i*, is a function of the injection valve area and is defined as follows:

$$\tau_c \ddot{m}_{in,i} + \dot{m}_{in,i} = \frac{k\rho_l C_f A_{v,in}\sqrt{P_s - P_i}}{c_p T_1} \tag{2.13}$$

where C_f is the valve discharge coefficient for the injection valves, $A_{v,in}$ is the valve area of the injection valve, τ_c is the time constant of the catalyst pack reaction dynamic, k is the lower heating value of the hot gas, ρ_l is the density of the liquid propellant, T_1 is the temperature at the inlet, c_p is the specific heat at constant pressure, and P_s is the upstream pressure as typically supplied in a blowdown fuel tank. It should be noted that the mass flow rate into the system only occurs for 60 degrees of rotation. Past this point, there is no more inlet flow, because the chamber is no longer exposed to the inlet. Again, (2.13) can be solved using Matlab performing two integrations to solve for the mass.

The equation for the mass flow rate out of the system can be derived from equations that are typical of pneumatic systems for isentropic flow of an ideal gas through a converging nozzle. Mass flow rate of any system can be described by the following:

$$\dot{m} = \rho_l A v \tag{2.14}$$

where ρ_l is the density of the fluid, A is the area of the fluid passage, and v is the velocity of the fluid. For mass flow rate out of the chamber, the area is simply the area at the outlet. An m-file was created to define the area of the outlet according to the rotor angle. The density of compressible fluid undergoing isentropic flow through a converging nozzle is defined by the following from [7]:

$$\frac{\rho_l}{\rho_{lo}} = \left\{ \frac{1}{1+\left[(\gamma-1)/2\right]Ma^2} \right\}^{\frac{1}{\gamma-1}} \tag{2.15}$$

where ρ_{lo} is the stagnate fluid density and *Ma* is the mach number which can be solved for using the following from [7]:

$$\frac{P}{P_o} = \left\{ \frac{1}{1+\left[(\gamma-1)/2\right]Ma^2} \right\}^{\frac{\gamma}{\gamma-1}} \tag{2.16}$$

where P_o is the stagnate fluid pressure. The velocity of the fluid can be defined by the following equation for the definition of mach number which also comes from [7]:

$$v = Ma\sqrt{RT\gamma} \tag{2.17}$$

By substituting Eqs. (2.15) - (2.17) into (2.14) the mass flow rate out may be defined by the following:

$$\dot{m}_{out,i} = \begin{cases} \sqrt{\frac{\gamma}{RT_i}\left(\frac{2}{\gamma+1}\right)^{\left(\frac{\gamma+1}{\gamma-1}\right)}} P_i A_{ex,i}(\theta) & \text{if } \frac{P_{atm}}{P_i} \le C_r \\ & \text{(choked)} \\ \sqrt{\frac{2\gamma}{RT_i(\gamma-1)}}\sqrt{1-\left(\frac{P_{atm}}{P_i}\right)^{\left(\frac{\gamma-1}{\gamma}\right)}} \cdots & \\ \cdots\times\left(\frac{P_{atm}}{P_i}\right)^{\left(\frac{1}{\gamma}\right)} P_i A_{ex,i}(\theta) & \text{otherwise} \\ & \text{(unchoked)} \end{cases} \tag{2.18}$$

where $A_{ex,I}$ is the exhaust valve area (as a function of the rotor angle) for each chamber, and C_r is the pressure ratio at which flow becomes choked (approximately 0.5). All equations used to derive the mass flow rate out are from [7].

Exhaust ports are present on the vane motor from 210 degrees through 330 degrees of rotation. Due to the fact that each chamber is 60 degrees in size, at least some mass flow rate out of a single chamber occurs from 210 to 390 degrees of rotation. It is desirable to have all of the working fluid removed from the system each rotation, so that no back pressures are created that could potentially cause noise, damage to the system or loss of efficiency.

Equations (2.9), (2.13), and (2.18) were solved simultaneously and substituted into (2.2) to solve for the torque created by the system. The parameters used are listed in

Table 1 and come from specifications given by Vanderbilt University for a hot gas vane motor that is currently being constructed and also from specifications of the hot

gas being used from [8].

Table 1 Vane motor parameters.

Symbol	Name	Quantity
R_R	Radius of Rotor	0.0143 m
R_S	Radius of Stator	0.0175 m
$A_{v,in}$	Valve Area	0.2047 cm^2
t	Vane thickness	3.175 mm
b_{load}	Viscous Rotational Damping	1.7e-4 kgm^2/s
T_1	Inlet Temperature	505.15 K
W	Width of Rotor/Stator	0.035 m
C_f	Valve Discharge Coefficient	0.78
γ	Ratio of Specific Heats	1.344
ρ_l	Density of Liquid Propellant	1000 kg/m^3
c_p	Specific Heat at Constant Pressure	1005 J/kg/K
τ	Time Constant	0.005 s
C_r	Pressure Ratio	0.5
J_{load}	Rotational Inertia	1.7e-4 kgm^2
k	Lower Heating Value of the Hot Gas	800 kJ/kg
m	Mass of Rotor	0.113 kg
m_v	Mass of Vane	0.0118 kg
P_{atm}	Atmospheric Pressure	101325 Pa
P_s	Supply Pressure	1.88 MPa
R	Gas Constant	287 J/kg/K

It was assumed that viscous rotational damping was present, so the torque created by this friction needed to be subtracted from the torque created by the working chambers. Other frictional forces are also present between the vane tips and the stator, but the effects of that friction will be addressed in a later chapter. Therefore, the total torque in the system may be defined as follows:

$$\begin{aligned} T_s(t) &= J_{load}\ddot{\theta} \\ &= \sum_{n=1}^{N} P_i(t)\left[A_f r_f \theta_f(t) - A_a r_a \theta_a(t) \right]_i - b_{load}\dot{\theta} \end{aligned} \tag{2.19}$$

where J_{load} is the rotational inertia, b_{load} is the viscous rotational damping. It should be noted that there is no load torque considered in Eqn. (2.19), so all simulations are for no load conditions. There are six separate chambers so a total of 24 equations need to be integrated to solve for the total torque in the system. Equations (2.13) and (2.19) need to be integrated twice in order to be solved. The integration was performed using Simulink software.

2.3 Simulation Results

The hot gas vane motor is driven by the forces created from pressurized hot

gas. Figure 6 displays the pressure in a single chamber once the device has reached a constant velocity.

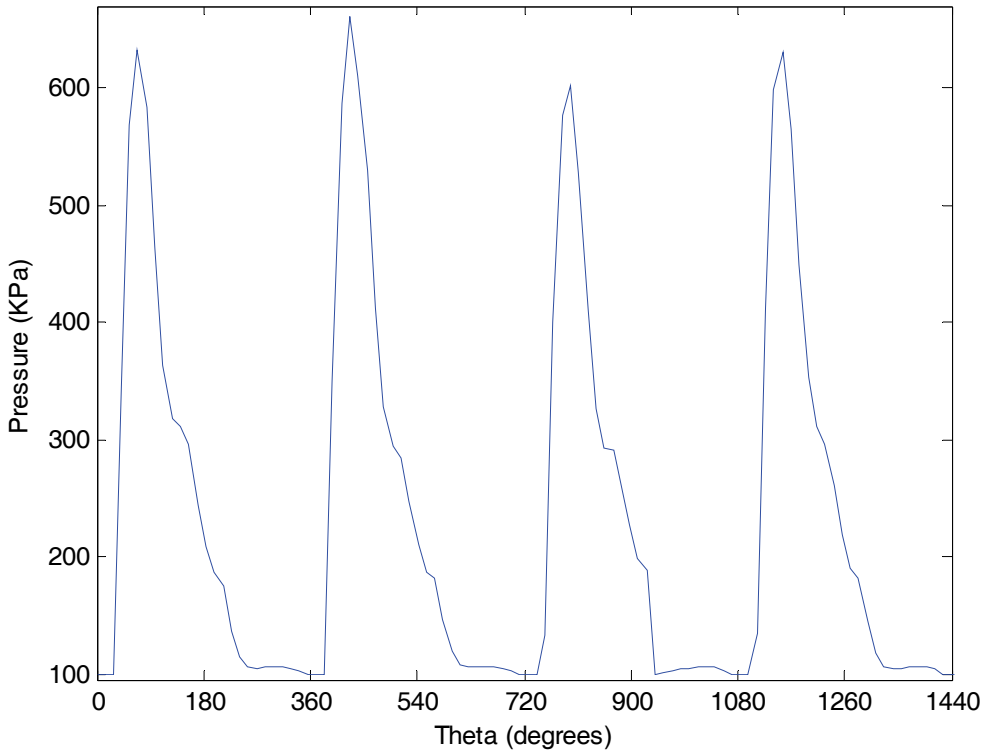

Figure 6. Pressure in a chamber at steady state.

There are pressure spikes once the device has rotated 30 degrees. This is the point at which the chamber is first exposed to the inlet port. This is also the instant when the chamber has its smallest volume. For a particular vane, the device is producing a positive torque from 30 to 210 degrees. Just prior to 210 degrees, the pressure is nearly at atmospheric pressure, and once the chamber reaches 210 degrees the pressure drops to atmospheric pressure. This is the point at which the chamber is exposed to the outlet ports and is no longer producing any torque. The pressure is reduced from 30 to 210 degrees due to the fact that the volume is increasing. Figure 7 displays the volume of a single chamber through two rotations.

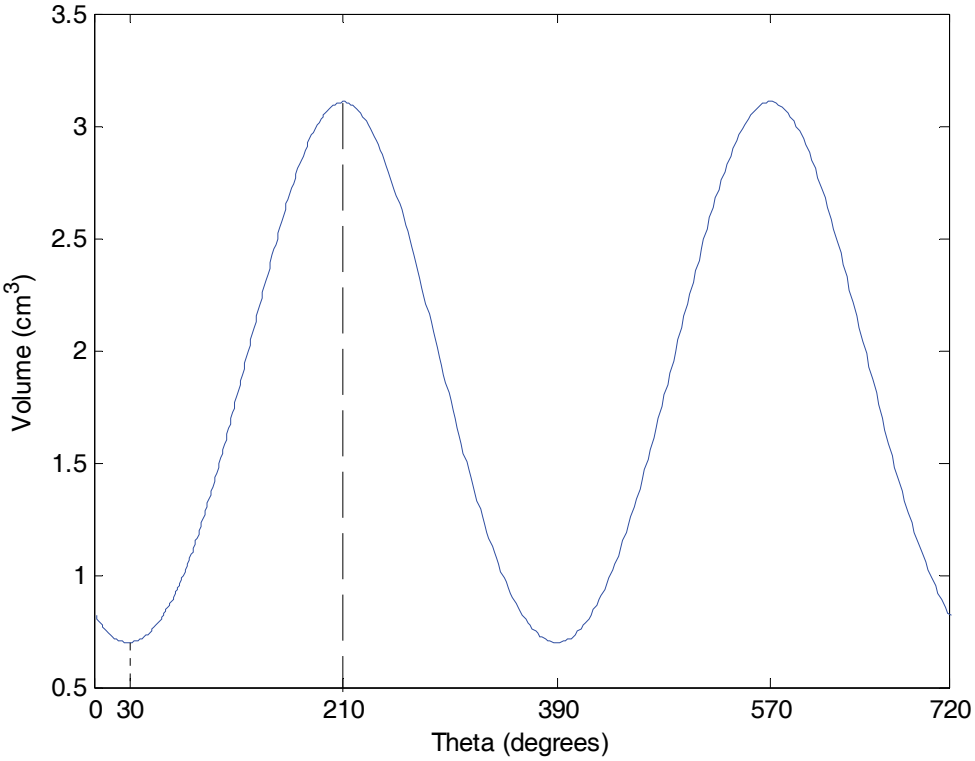

Figure 7. Volume through two rotations.

The minimum volume occurs at 30 degrees of rotation, while the maximum volume occurs at 210 degrees. This is why the inlet and exhaust ports are positioned at 30 and 210 degrees respectively. In these positions the maximum amount of torque is produced for a six chambered hot gas vane motor. Figure 8 displays the net torque of the hot gas vane motor.

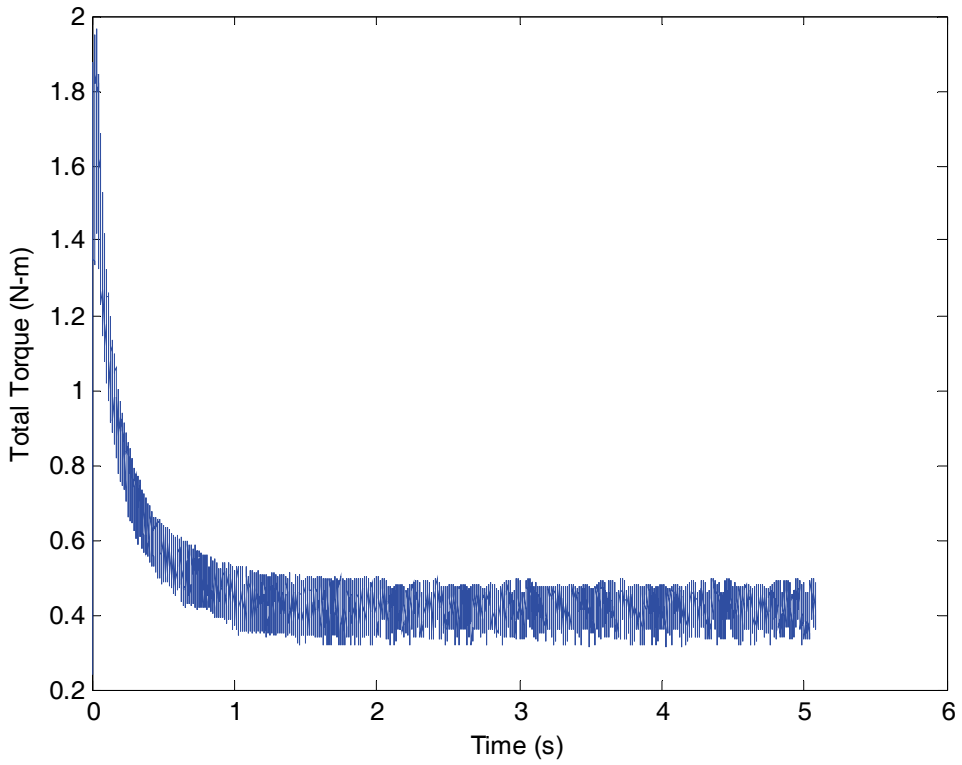

Figure 8. Total Torque of the hot gas vane motor.

Ultimately, the torque should be reduced to zero at steady state. Figure 8 only displays the amount of torque that is significant. Once, the torque reached a negligible amount, the simulation was stopped. The total torque decreases as the device approaches steady state. This is partly due to the increasing viscous friction, and also due to the fact that the motor is rotating at a much higher speed.

The results obtained using the aforementioned modeling equations are a good starting point for the hot gas vane motor. The main discrepancy in the results is the high angular velocity. The following figure displays the angular velocity of the hot gas vane motor.

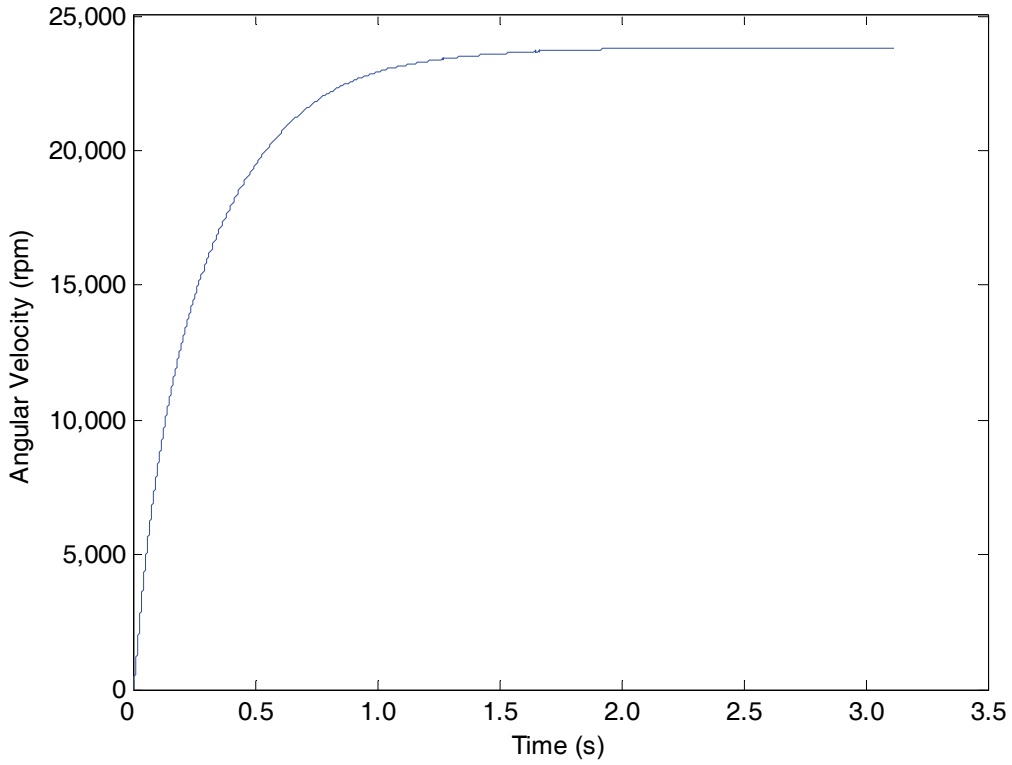

Figure 9. Angular velocity verses time for the hot gas vane motor.

Hot gas vane motors are capable of high rpm's (up to 13,000 rpm), especially lightweight motors such as the one being addressed by this work. The results from the model are nearly 25,000 rpm, which suggests that adjustments need to be made to the model. The main component that is missing from the model is a valid model for the friction torque. In order to improve the accuracy of the model, an appropriate model of the friction present on the sides and tips of the vanes needs to be added.

Chapter 3

Friction Model

3.1 Derivation of Friction Model

A valid model of friction is needed to improve the accuracy of the hot gas vane motor model. Research from Guoyuan, Qisen, and Yongzhang [9] on a similar device shows that the main source of friction within the hot gas vane motor is between the vane tips and the stator. Their research shows that the tip friction accounts for nearly 90% of the total friction within the system. Friction is also present where the sides of the vanes come in contact with the stator, but the majority of friction losses occur at the tip. The focus of this chapter will be to develop a model of the friction between the tips of the vanes and the stator. The friction within the system was solved for using fundamental dynamics equations. By determining the centripetal and rotational acceleration of each vane, the contact force between the vane and stator could be determined. If the friction coefficient between the vane and the stator is known, then the friction force may be solved for. It was assumed that each vane could be treated as a point mass in a rotating coordinate frame centered at the rotor. The acceleration, *a*, of a point, *p*, on the tip of each vane can be defined by the following from [10],

$$\bar{a} = \ddot{\bar{R}} + \dot{\bar{\omega}} \times \bar{l} + \bar{\omega} \times \left(\bar{\omega} \times \bar{l} \right) + 2\bar{\omega} \times \dot{\bar{l}}_r + \ddot{\bar{l}}_r \tag{3.1}$$

where $\ddot{\bar{R}}$ is the absolute acceleration of the coordinate frame rotating about a point, $\bar{\omega}$ is the absolute angular velocity of the rotor, $\dot{\bar{\omega}}$ is the absolute angular acceleration of the rotor, $\bar{l}$ is the radius to the edge of the stator and $\dot{\bar{l}}_r$ and $\ddot{\bar{l}}_r$ are the relative

velocity and acceleration of a single vane to the coordinate frame respectively. Figure 10 displays the coordinate frame used to solve for the acceleration of each vane. It should be noted that the coordinate frame is rotating about a fixed point so there is no offset distance, *R*, between the center of rotation and the coordinate frame. The **ij** coordinate frame is intended to follow the path of a single vane as it rotates about the **xy** coordinate frame.

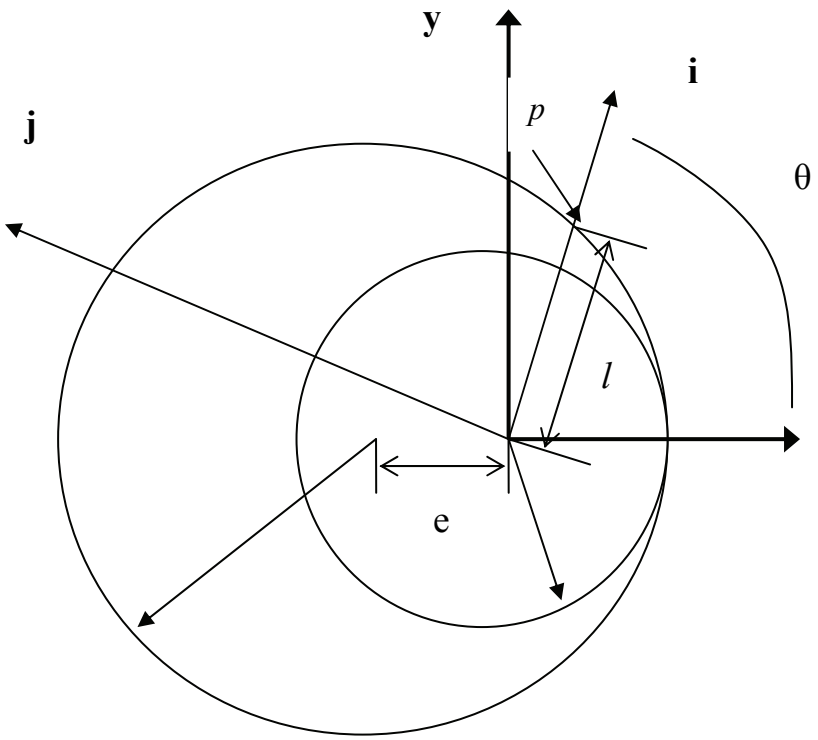

Figure 10. Coordinate frames used to define acceleration.

As was determined earlier in Chapter 2, the radial distance from the center of the rotor to the stator in the **i** direction is defined as follows:

$$\bar{l} = -e\cos(\theta) + \sqrt{R_S{}^2 - (e\sin(\theta))^2}\,\hat{i} \tag{3.2}$$

Once $\bar{l}$ is known, Eq. (3.2) may be used to determine the acceleration. The

components of (3.1) are defined by the following,

$$\ddot{\bar{R}} = 0 \tag{3.3}$$

$$\begin{aligned} \dot{\bar{\omega}} \times \bar{l} &= \left(\dot{\omega}\hat{k}\right) \times \left(-e\cos(\theta) + \sqrt{R_S{}^2 - (e\sin(\theta))^2}\,\hat{i}\right) \\ &= \dot{\omega}\left(-e\cos(\theta) + \sqrt{R_S{}^2 - (e\sin(\theta))^2}\right)\hat{j} \end{aligned} \tag{3.4}$$

$$\begin{aligned} \bar{\omega} \times \left(\bar{\omega} \times \bar{l}\right) &= \left(\omega\,\hat{k}\right) \times \\ &\quad \left(\left(\omega\,\hat{k}\right) \times \left(-e\cos(\theta) + \sqrt{R_S{}^2 - (e\sin(\theta))^2}\right)\hat{i}\right) \\ &= -\omega^2\left(-e\cos(\theta) + \sqrt{R_S{}^2 - (e\sin(\theta))^2}\right)\hat{i} \end{aligned} \tag{3.5}$$

$$\begin{aligned} 2\bar{\omega} \times \dot{\bar{l}}_r &= 2\left(\omega\,\hat{k}\right) \times \left(e\omega\sin(\theta) - \frac{1/2e^2\omega\sin(2\theta)}{\sqrt{\left(R_S{}^2 - \left(e\sin(\theta)^2\right)\right)}}\hat{i}\right) \\ &= 2\omega^2\left(e\sin(\theta) - \frac{1/2e^2\sin(2\theta)}{\sqrt{\left(R_S{}^2 - \left(e\sin(\theta)^2\right)\right)}}\right)\hat{j} \end{aligned} \tag{3.6}$$

$$\begin{aligned} \ddot{\bar{l}}_r &= e\omega^2\cos(\theta) + e\dot{\omega}\sin(\theta) \\ &\quad -1/2e^2\left[\begin{array}{c} \dfrac{\left(2\omega^2\cos(2\theta)\right)}{\sqrt{\left(R_S{}^2 - \left(e\sin(\theta)^2\right)\right)}} + \dfrac{\dot{\omega}\sin(2\theta)}{\sqrt{\left(R_S{}^2 - \left(e\sin(\theta)^2\right)\right)}} + \\ \dfrac{1/2e^2\omega^2\sin(2\theta)}{\left(R_S{}^2 - \left(e\sin(\theta)\right)^2\right)^{3/2}} \end{array}\right]\hat{i} \end{aligned} \tag{3.7}$$

It should be noted that only the acceleration in the **i** direction is needed in order to determine the normal force. Therefore, only Eqs. (3.7) and (3.5) need to be considered and the acceleration in the **i** direction is defined by the following:

$$\bar{a}_i = \bar{\omega} \times \left(\bar{\omega} \times \bar{l}\right) + \ddot{\bar{l}}_r \tag{3.8}$$

If the rotor of the vane motor was not offset from the stator then only, Eq. (3.5) would need to be considered. However, since this is not the case, the relative motion of the vanes moving in and out of their respective slots needs to be taken into consideration. This motion does add a sizable amount of acceleration. The added acceleration causes the total acceleration to oscillate more since the vanes are accelerating in and out of their slots. A comparison of acceleration with and without the added relative acceleration term may be seen in Figure 11.

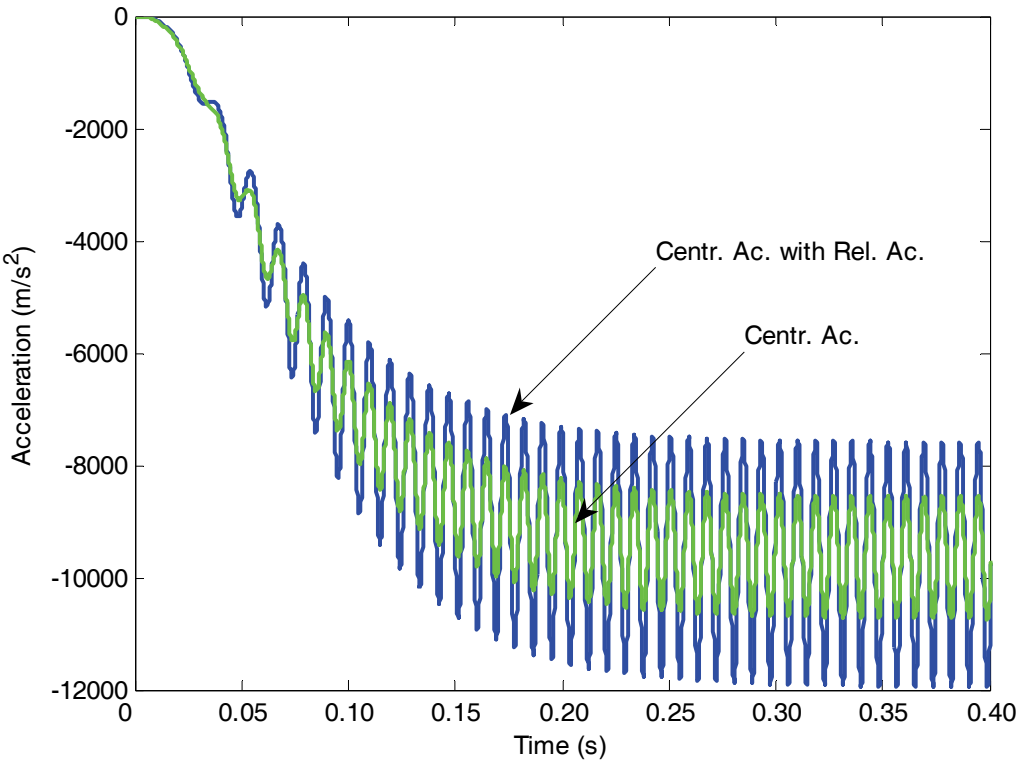

Figure 11. Acceleration of a single vane throughout operation.

Once total acceleration is known, the normal force due to acceleration, F_{Na}, may be determined by using trigonometry and summing the forces in the **i** direction. From Figure 12, it can be seen that the sum of the forces in the **i** direction is given by the following,

$$\sum F_i = m_v a_i = F_{Na}\cos(\beta) - \sin(\beta)F_f \tag{3.9}$$

where m_v is the mass of the vane, a_i is the **i** component of the vane acceleration, β is the angle between the direction of the normal force and the **i** direction, and F_f is the friction force between the rotor and stator and is defined by the following basic equation:

$$F_f = \mu F_{Na} \tag{3.10}$$

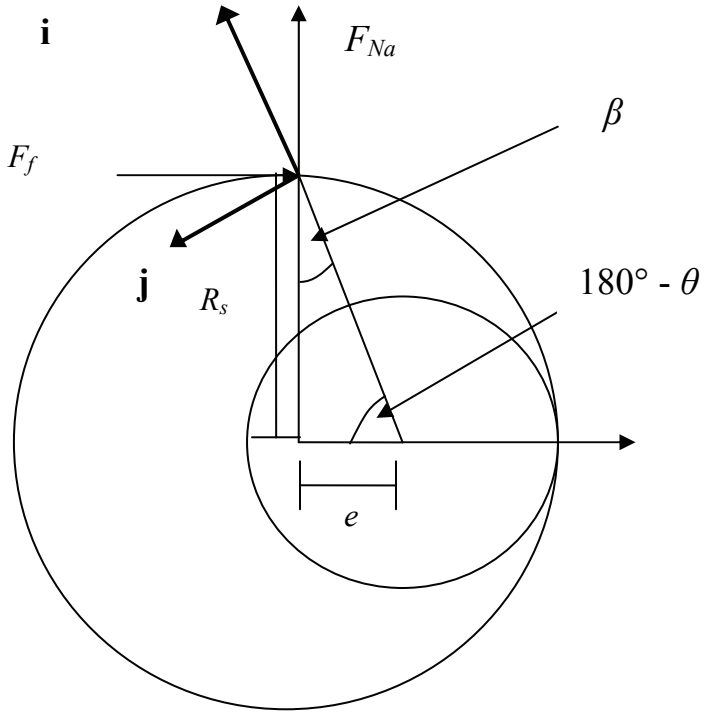

Figure 12. Orientation of the normal force and the friction force on the vane motor.

If the angle β is small then Eq. (3.9) may be reduced to the following:

$$F_{Na} \approx m_v a_i \tag{3.11}$$

This is due to the fact that for small angles, cosine is approximately one and sine is approximately zero. The angle, β, is a function of the angular position of a vane, θ,

and the geometry of the hot gas vane motor. From the law of sines, it may be shown that the equation for β is:

$$\beta = \sin^{-1}\left(\frac{\sin\left(180^{\circ} - \theta\right)}{R_s} e\right) \tag{3.12}$$

At maximum the angle, β, is only 10 degrees as seen in Figure 13. Therefore, the small angle approximation used in Eqn. (3.11) will be used for the rest of this work.

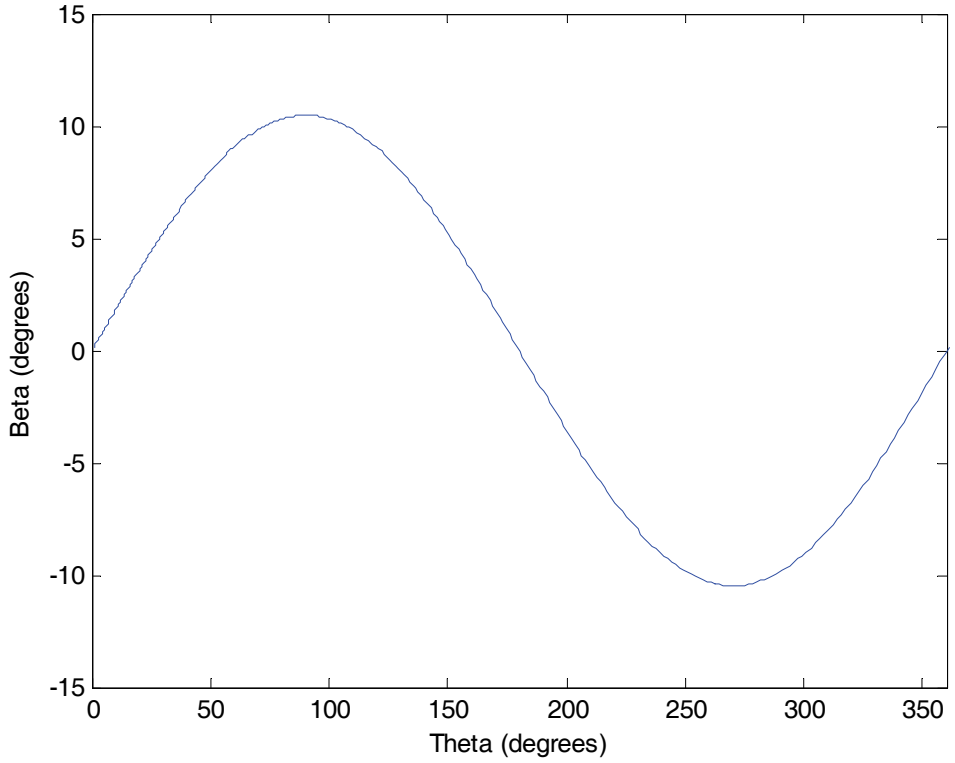

Figure 13. The angle β throughout a single rotation.

In order to determine the friction force, the normal force and the coefficient of friction need to be determined. The coefficient of friction for sliding surfaces may be determined using the Stribeck Curve. A mathematical model for this curve has been

suggested in previous work [4] and is presented here as

$$\mu = \mu' \,\mathrm{Exp}\left(-\alpha \frac{\eta_f \, l \, \omega}{N'}\right) + \varepsilon \sqrt{\frac{\eta_f \, l \, \omega}{N'}} \tag{3.13}$$

where μ' is the boundary lubrication coefficient of friction, α and ε are coefficients that are used to fit the Stribeck Curve, η_f is the absolute fluid viscosity of the gas within the motor, N' is the load per unit width at the sliding interface, and other parameters have been defined previously. The load per unit width, N', is simply the normal force divided by the width of the vane, *W*.

$$N' = \frac{F_{na}}{W} \tag{3.14}$$

According to Manring [11], the start of the Stribeck curve describes the beginning of the operation where the angular velocity and subsequently the sliding velocities are low. Figure 14 displays a typical Stribeck curve.

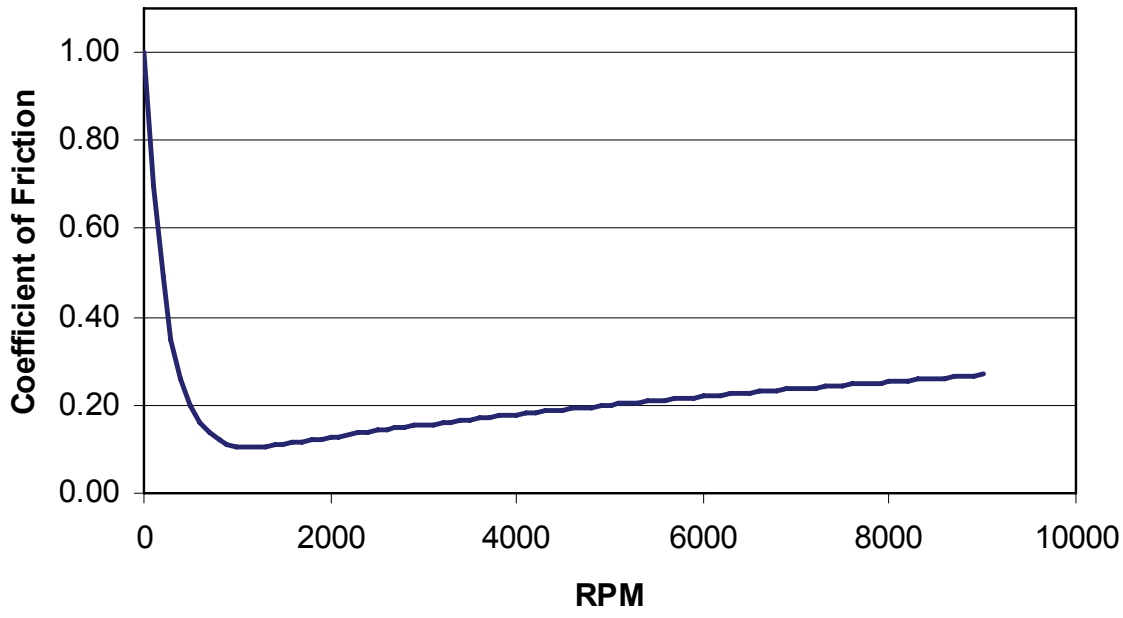

Figure 14. Typical Stribeck curve.

At the beginning of the operation the vanes are fully in contact with the stator. When the velocity is increased, mixed lubrication occurs and the vanes are only partly in contact with the stator so the friction coefficient is reduced. The final phase of the Stribeck curve describes the fully hydrodynamic zone of the operation where the surfaces are fully separated by a film of fluid and friction results from shearing the fluid itself. At this time it is unknown if there is significant liquid in the motor to support hydrodynamic lubrication.

Now that the friction coefficient and the normal force have been defined, the friction force may be solved for using Eq. (3.10). The goal of obtaining the friction force between the vane tip and the stator is to determine the amount of torque that is created by the friction. Torque is defined as the product between a force and the perpendicular distance from the center of rotation. For the hot gas vane motor the friction torque is defined as follows:

$$T_f = l \bullet F_f \tag{3.15}$$

where l is the distance from the center of rotation to the edge of the stator as defined by Eq. (3.2). Since it was assumed that the angle β is small, it is also assumed that F_f is always perpendicular to l. Therefore, a scalar multiplication is used in Eq. (3.15) rather than a cross product multiplication.

During operation, six separate vanes are rotating, which means that six separate torques are created. Solving for six separate friction torques greatly increases the calculation effort of the simulation. An attempt was made to reduce the simulation effort by computing the average friction torque during operation. It was

assumed that the friction torque could be approximated as the average friction torque during one rotation which is defined by the following:

$$\bar{T}_f = \frac{n}{2\pi}\int_0^{2\pi} T_f \, d\theta \tag{3.16}$$

where n is the number of vanes. A comparison of the results between average friction torque and the actual calculated friction torque is presented in Section 3.2. The net torque on the rotor, including the torque created by the pressurized chambers and both viscous friction and the friction between the vane tips and the stator, is now defined as:

$$T_s(t) = \sum_1^n P_i(t)\left[A_f r_f \theta_f(t) - A_a r_a \theta_a(t) \right]_i - b\dot{\theta} - T_f \tag{3.17}$$

3.2 Simulation Results Including Friction Torque

The coefficient of friction between the vane tips and the stator was solved for using a Stribeck curve. Figure 15 displays how the coefficient of friction changes with time.

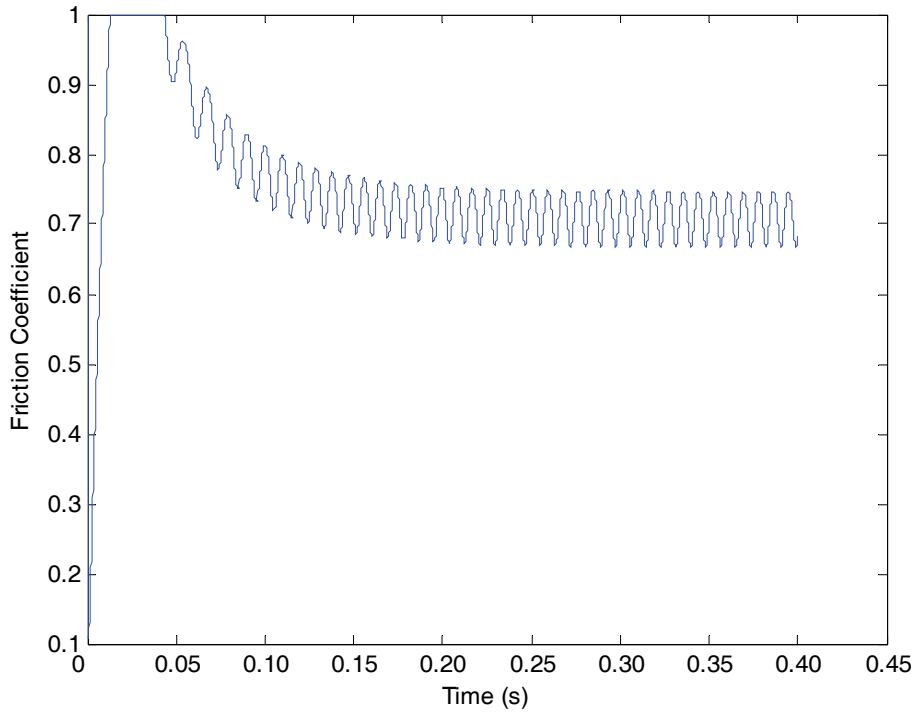

Figure 15. Coefficient of friction verses time.

Figure 15 shows a typical response of a system with Stribeck friction. The coefficient of friction is very high during start up due to low velocities. This is the point at which the vane is fully engaged with the stator. The coefficient of friction is 1 so the friction force is the amount of normal force. Then, the coefficient is decreased as the angular velocity increases. This is a point of mixed lubrication. Once the angular velocity has increased enough the coefficient of friction stops decreasing and then increases slightly more until it reaches a steady state value at a constant velocity. This is the fully hydrodynamic zone of the Stribeck Curve which assumes a thin film of fluid is present between the rotor and stator. In this case the coefficient levels out at about 0.725. This is a relatively high coefficient of friction. This is mainly due to the low normal force. The normal force is displayed in Figure 16.

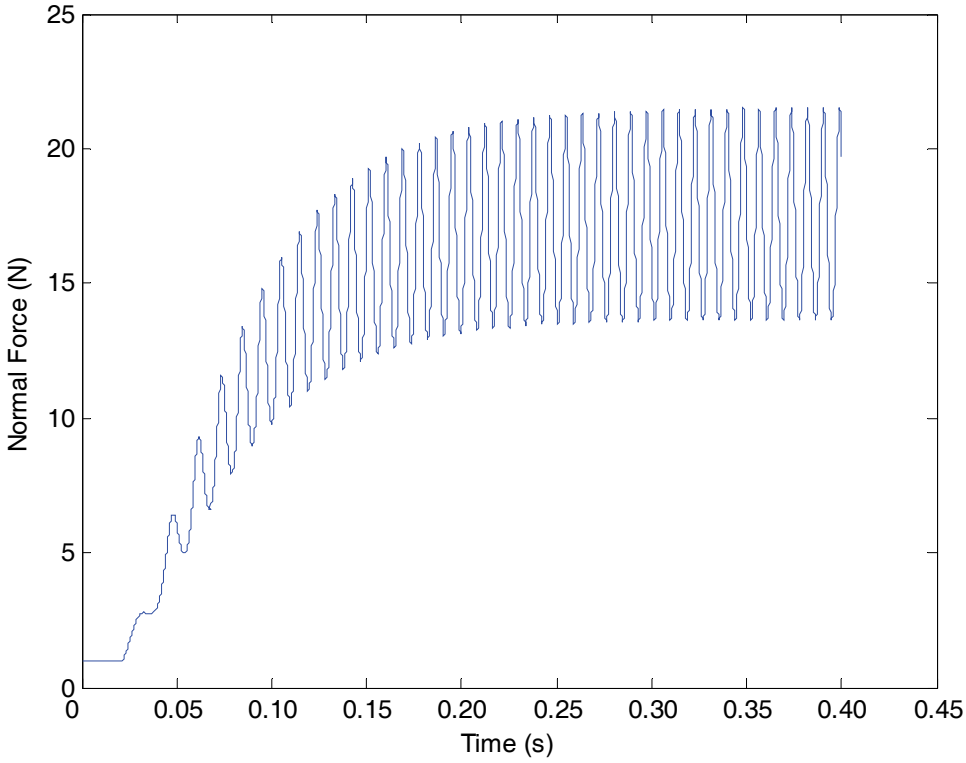

Figure 16. Normal force between a singular vane tip and the stator.

For now, it is assumed that the only factor that affects the normal force is the acceleration of the vane. The normal force increases during operation due to the fact that the acceleration of the vane is increasing as the angular velocity increases. There is a lot of oscillation in the normal force, because the vanes of the motor accelerate in and out of their respective slots throughout operation.

The friction torque in the system was solved for using two separate methods. An average friction torque was determined using integration as seen in Eqn. (3.16). Also, the actual friction torque was solved for by solving for the friction created by each of the six vanes separately by using Eqn. (3.15) for each individual vane and summing the results. Figure 17 displays both the average and actual friction torques.

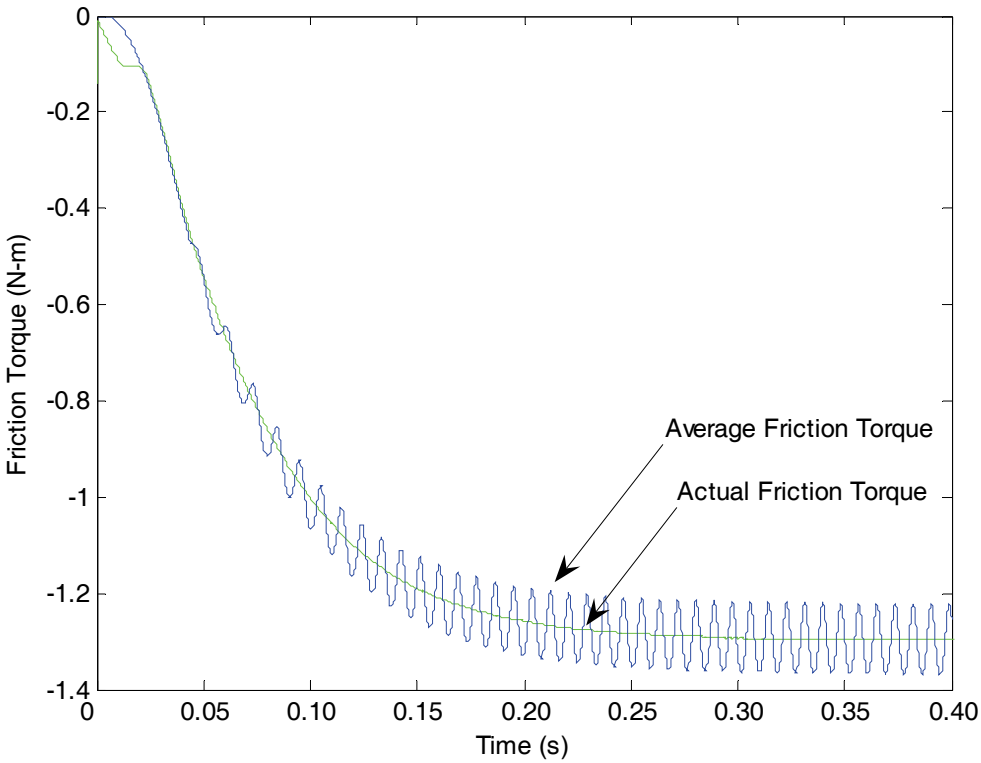

Figure 17. Average and actual friction torque of the hot gas vane motor.

Using integration to solve for friction torque provides for a much faster calculation, but does not provide the most accurate results. The integrator used, solves for the friction torque by solving for the amount of torque created by a single vane during a single rotation and then averaging the total torque that would be created by six separate vanes. The integration integrates at each time step, so it is as if one vane that is six times the size of a single vane is rotating throughout operation. During rotation, the friction torque of each individual vane will increase and decrease due to the fact that the normal force is increasing and decreasing depending on the position of the vane which may be seen in Figure 16. The oscillation affect of the normal force becomes magnified when the average friction torque is solved for. The actual friction torque also oscillates slightly, but it oscillates at a much lower

amplitude since the friction torque of each vane is solved for separately and then summed together. The advantage to using an average friction torque is a decrease in computational effort, but an undesirable oscillatory affect is created. For higher accuracy, the friction torque of each vane should be solved for separately. In this work, the friction torque was solved for by solving for the friction torque of each vane separately for accuracy.

As was previously stated, the friction coefficient decreases during operation while the normal force increases as speed increases. Because, the normal force increases more than the friction coefficient decreases, the overall friction torque increases during operation as seen in Figure 17. The friction torque works against the direction of motion, which is why it is negative. As the friction torque increases with increasing angular velocity, the net torque on the system decreases as seen in Figure 18.

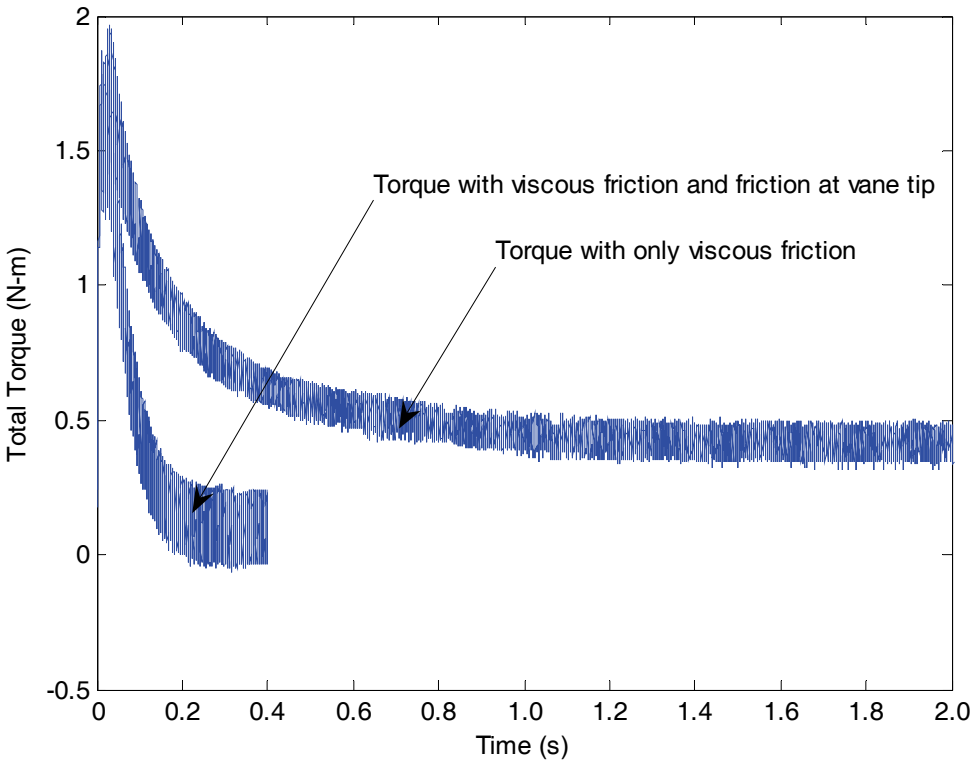

Figure 18. Net torque of the system.

Both torques should be reduced to zero. Only the significant portion of torque is presented in Figure 18. Once the angular velocity stopped increasing at a significant rate the simulation was stopped. When only viscous friction was present on the device, the net torque required more time to reach steady state. Without friction on the vane tips the device takes almost 2 seconds to reach steady state, whereas with friction on the vane tips, the device takes only about 0.4s. The added friction torque from friction between the stator and the vane tips is what slows down the device allowing a steady state to be reached at a faster rate. In both cases, the velocity is still increasing slightly, but the rate at which it is increasing is very slow, so it was assumed that a steady state had been reached.

Because the friction torque is increased when Stribeck friction is used, the overall angular velocity is also decreased. A problem with the simulation discussed in Chapter 2 was that the angular velocity was unrealistically high. This was the motivation for developing a more detailed description of the friction. The following figure displays the angular velocity of the hot gas vane motor.

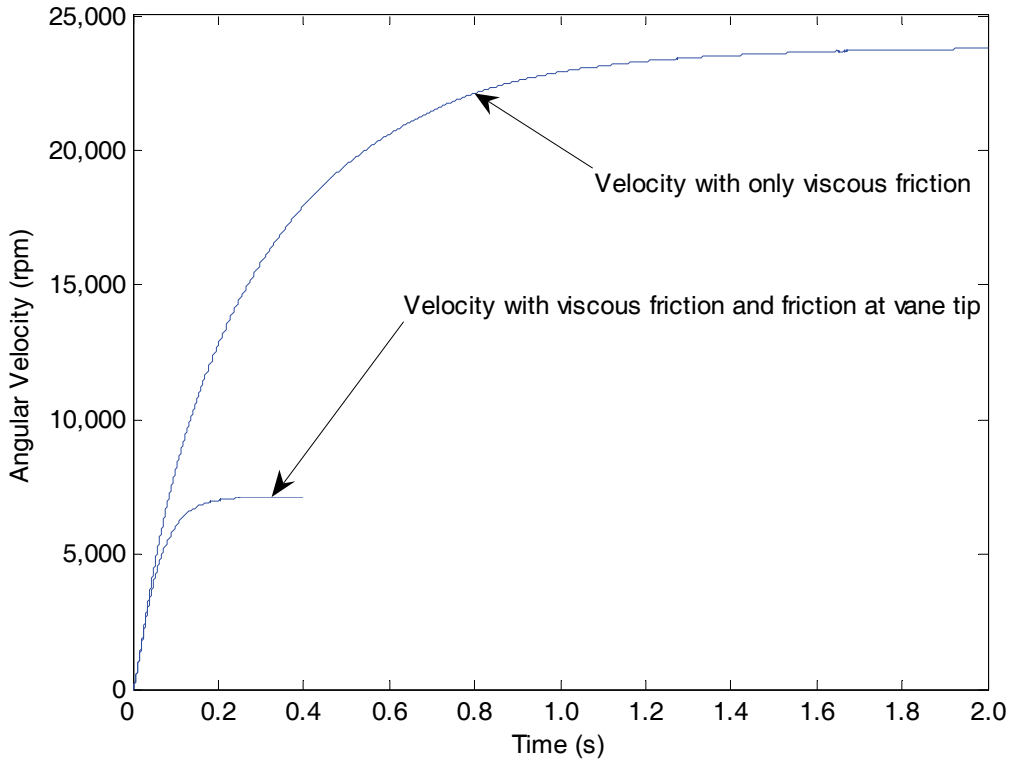

Figure 19. Angular velocity of the hot gas vane motor.

The angular velocity has been greatly reduced due to the presence of friction. Also, it may be seen that with friction at the vane tips present the device reaches a steady state velocity a lot faster. With only viscous friction included, the steady state angular velocity reached nearly 25,000 rpm, whereas with both viscous friction and friction at the vane tip, the angular velocity is closer to 7,100 rpm. This is a much

more reasonable level of angular velocity. However, there is one factor that has yet to be considered, and that is the pressure on the ends of the vane. Depending on how the hot gas vane motor is designed, there may be a significant amount of pressure on the back end of the vanes, which would in turn increase the normal force and also the amount of friction on the tip of each vane.

Chapter 4

Pressure Model

4.1 Discussion of Pressure Model

It was shown in the previous chapter that the amount of friction on the end of the vanes has a significant affect on the operation of the hot gas vane motor. The friction force is a function of the normal force between the vane tips and the stator. Increasing the normal force on the end of the vane increases the friction between the vane and the stator, but it also ensures the vane stays in contact with the stator so that minimum leakage occurs between chambers. The focus of this chapter will be to discuss the affects of pressure on the ends of the vane.

In order to ensure a tight seal between pressurized chambers and reduce the possibility of leakage, the backside of each vane is pressurized by the preceding chamber. Figure 20 displays the rotor along with the vane pressurization ports.

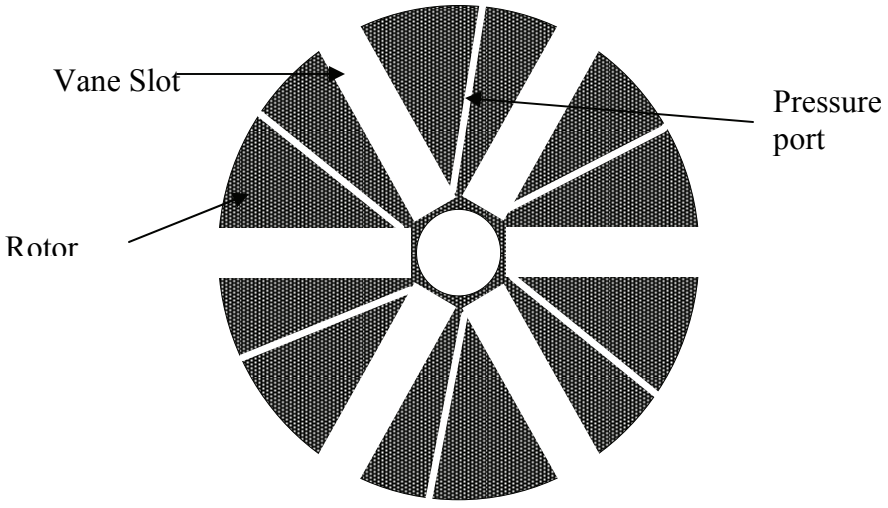

Figure 20. Rotor and vane pressurization ports.

It should be noted that the vane does not need to be in contact with the stator for the exhaust phase of operation. The chambers are not pressurized at this point and no torque is created, so no seal is required between the vane and stator. Also, the vane is not pressurized during the exhaust phase of the operation, between 210 and 30 degrees, since the pressure is reduced to atmospheric at this point. This means that the pressure does not affect the amount of friction within the system during the exhaust phase of operation since pressure forces on the ends of the vane are equalized.

During the working phase of operation, between 30 and 210 degrees, the vane is pressurized to counteract pressure forces on the tip of the vane so extra friction is created. The amount of pressure on the vane tip depends on the shape of the vane. The two most likely shapes of a vane would be either a straight-edged vane or a rounded vane. A straight-edged vane will eventually become rounded due to wear caused by the contact between the vane tip and the stator. This work will consider both conditions for a vane tip.

4.2 Straight-edged Vane Tip Pressure Calculation

The straight edged vane will be considered first. The amount of pressure on the tip of the vane is dependant on the exposed area on the tip of the vane and is therefore dependant on the orientation of a particular vane. For a straight-edged vane, it is assumed that the vane is either tilted forward in its slot, exposing the vane to the pressure of the leading chamber, or else the vane is tilted back in its slot exposing the vane to the pressure of the lagging chamber.

Figure **21** displays the orientation of a straight-edge vane as it is tilted both forward and backwards.

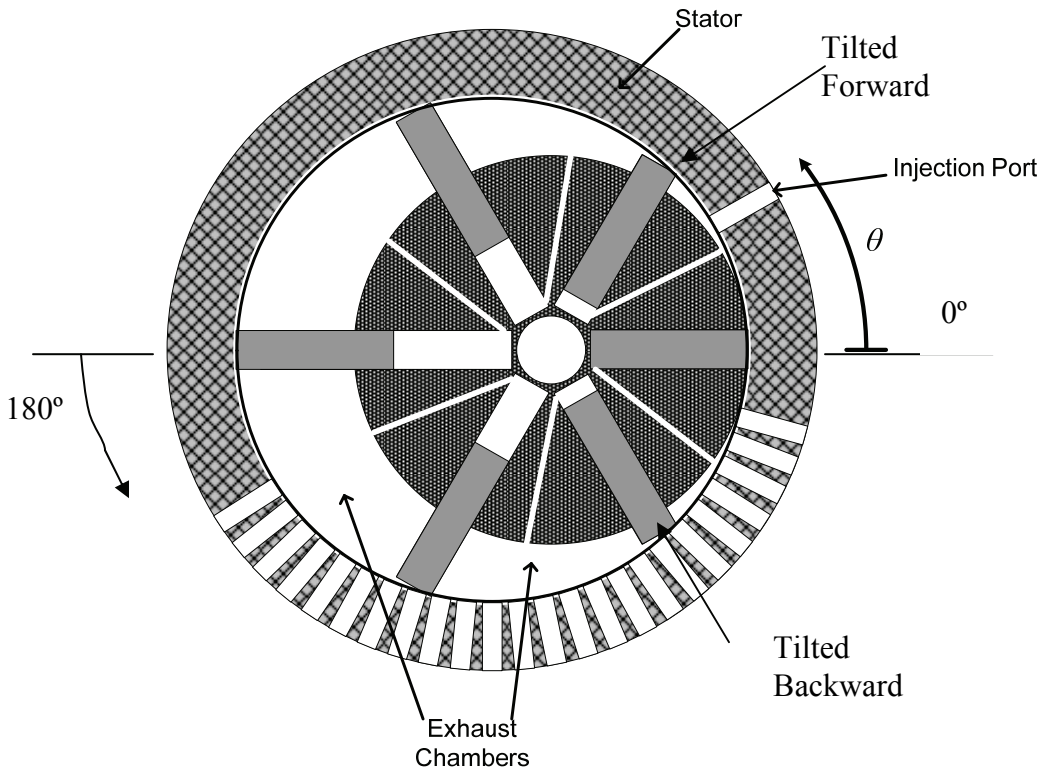

Figure 21. Orientation of a straight-edge vane.

Due to the geometry of the hot gas vane motor, the vane should be tilted forward from 0 to 180 degrees. Therefore, for the first half of operation the vane tip is exposed to the leading chamber's pressure. From 180 to 360 degrees the vane is tilted slightly back so that the vane tip is exposed to the pressure in the preceding

chamber. The total force due to pressure from 180 to 360 degrees is zero, since the backside of the vane is also pressurized by the lagging chamber. During the exhaust phase from 210 to 30 degrees, it is irrelevant which chamber the vane is exposed to since the pressures are both atmospheric. From 0 to 30 degrees, no friction is added due to pressure since the pressures on both ends of the vane are identical.

From 30 to 180 degrees, a net force is created due to the pressure difference between the ends of the vanes. The added force increases the normal force on a particular vane, thus increasing the friction torque. The added normal force due to pressure for a single vane in the *i*th chamber is defined by the following:

$$F_{np} = \begin{cases} 0 & 0^\circ < \theta < 30^\circ \\ \left(P_i - P_{i+1}\right) A_{vi} & 30^\circ < \theta < 180^\circ \\ 0 & 180^\circ < \theta < 360^\circ \end{cases} \tag{4.1}$$

where A_{vi} is the area of the tip of the *i*th vane, and P_i and P_{i+1} are the pressures in chambers *i* and *i+1* respectively. Chapter 3 discussed how to solve for the normal and friction forces caused by centripetal forces. By adding the normal force due to pressure to the normal force due to centripetal and relative forces and multiplying by the moment arm, a new term for frictional torque of a single vane may be computed.

$$T_f = l \times \left(F_{na} + F_{np}\right) \mu \tag{4.2}$$

The total friction torque within the system is the sum of the friction torques from each individual vane and the viscous friction. The net torque on the system, including both viscous friction and the newly defined friction between the vane tips and the stator, is defined as:

$$T_s(t) = \sum_1^n P_i(t) \left[A_f r_f \theta_f(t) - A_a r_a \theta_a(t) \right]_i - b\dot{\theta} - T_f \tag{4.3}$$

4.3 Rounded Vane Tip Pressure Calculation

For a rounded vane tip, the total pressure on the vane is slightly different than a straight-edged vane. For a rounded end, the actual position of the contact point between the vane tip and the stator is slightly off center, but for simplicity it was assumed that the center of the vane would be in contact with stator at all times. Therefore, half of the vane tip is exposed to the leading chamber's pressure and the other half of the vane tip is exposed to the lagging chamber's pressure. Figure 22 displays the orientation of a single rounded edge vane.

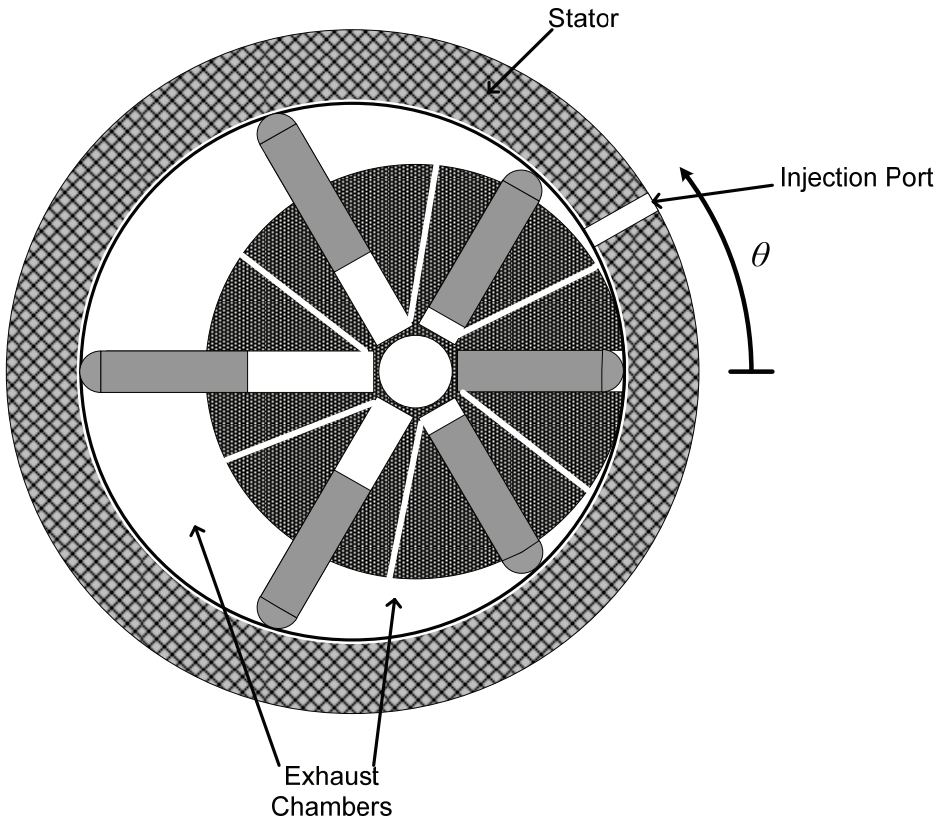

Figure 22. Orientation of a rounded edge vane.

The added normal force due to pressure for a single vane in the *i*th chamber is the difference between the force on the back of the vane and force on the tip of the vane and is defined by the following:

$$F_{np} = P_i A_{vi} - \left(1/2 P_i A_{vi} + 1/2 P_{i+1} A_{vi}\right) \tag{4.4}$$

where A_{vi} is the area of the tip of the *i*th vane, and P_i and P_{i+1} are the pressures in chambers *i* and *i+1* respectively. Equation (4.4) may now be substituted into Eq. (4.2) to solve for the friction torque. The total torque may again be solved for using Eq. (4.3).

4.4 Results

The purpose of channeling pressure to the backside of the vane is to counteract the pressure forces on the tip of the vane. The pressure on the backside should be larger than the pressure on the tip of the vane which means the overall normal force between the vane tip and the stator increases. In order to operate properly the vanes need to be pressurized to ensure the vanes never lose contact with the stator. The simulation of a hot gas vane motor running without pressure on the vane ends was presented to compare the affects of centripetal forces verses pressure forces on the performance of the hot gas vane motor. A plot of normal forces for the three cases that have been discussed, rounded-edge vane tip, straight-edge vane tip, and an unpressurized vane, is displayed in Figure 23.

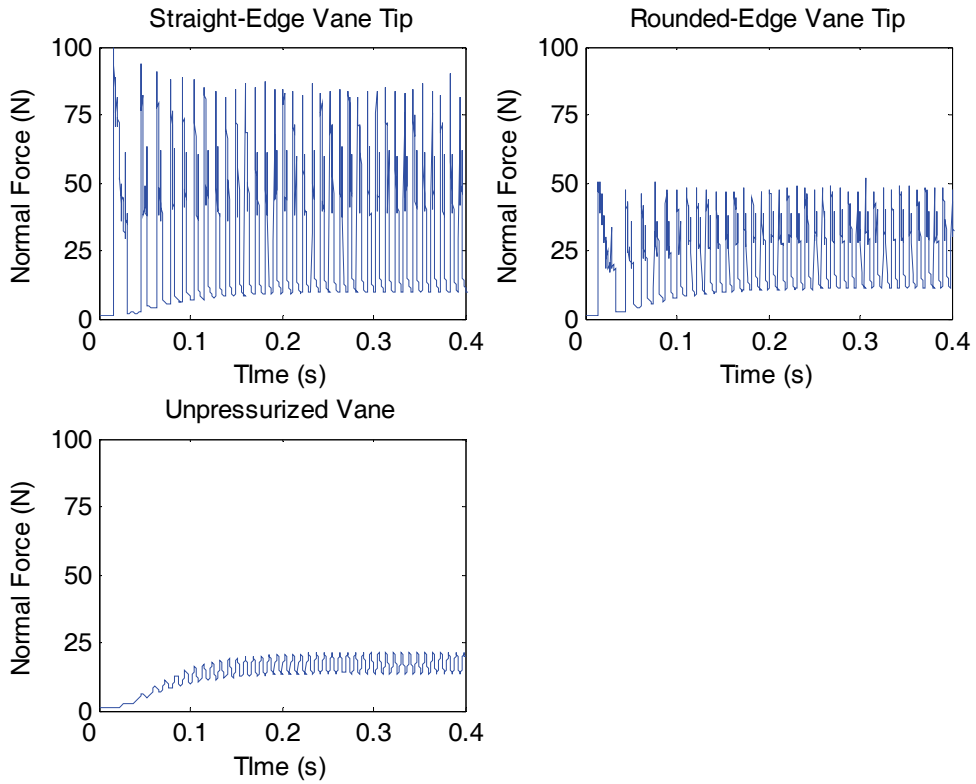

Figure 23. Comparison plots of the normal forces on a single vane.

Compared to the case where no pressure is present on the ends of the vane, the normal force has increased considerably. All three cases include the normal force created from centripetal acceleration. The normal force for the cases with pressure forces considered oscillates more than the case without pressure considered. Throughout operation the vane goes from a pressurized state where pressure forces are high to an unpressurized state where pressure forces are negated. A net increase in normal force occurs due to the added pressure forces during the first half of rotation. Both the rounded-edge vane and the straight-edge vane have high normal forces, but the straight-edge vane has a higher average normal force. The straight-edge vane has an average normal force of 29 N and a peak normal force of 90 N, wheras the rounded edge vane has an average normal force of 22 N and a peak

normal force of 51 N. The straight-edge vane is completely exposed to the lower pressure leading chamber. As a result, the pressure difference between the back of the vane and the tip of the vane should be much higher than that of the rounded edge vane. Approximately half of the rounded edge vane is exposed to the lower pressure leading chamber, so the pressure difference between the vane ends should be about half that of the straight-edge case.

It was shown in the previous chapter that increasing the normal force decreases the coefficient of friction, which is a trait of the Stribeck Curve. Figure 24 displays the coefficient of friction for the three cases under discussion.

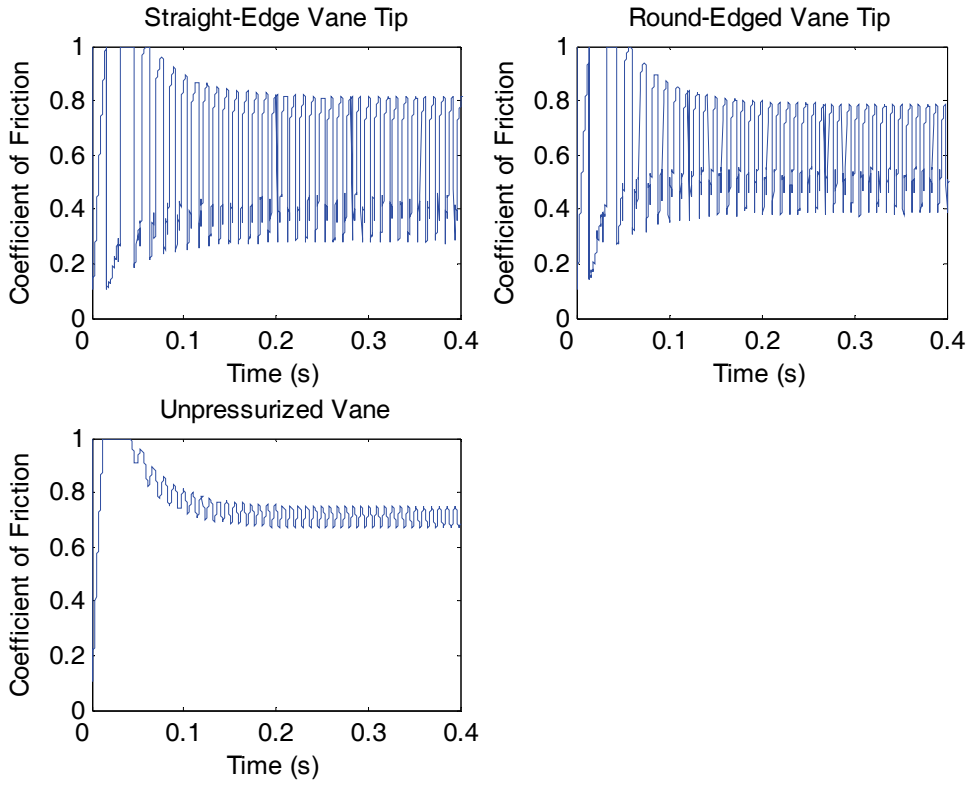

Figure 24. Comparison of the coefficient of friction of a single vane.

As is expected, the cases with pressure forces included have a lower coefficient of friction, than the case without pressure force due to the higher normal

forces. The friction coefficient oscillates, because the normal force oscillates due to the vane entering and exiting the pressurized portion of operation. When the vane is in the exhaust phase and no pressure forces are present, the coefficient of friction is only based on centripetal forces, and is fairly close to the results from the unpressurized case. Without pressure, the coefficient of friction at steady state was roughly 0.7. For a straight-edge vane tip, the coefficient of friction oscillates, but on average the coefficient of friction is about 0.4. The rounded edge vane tip has a slightly higher average coefficient of friction, 0.5, due to the lower normal forces.

Higher normal forces cause the total friction force to increases. Figure 25 displays the total friction torque of the hot gas vane motor.

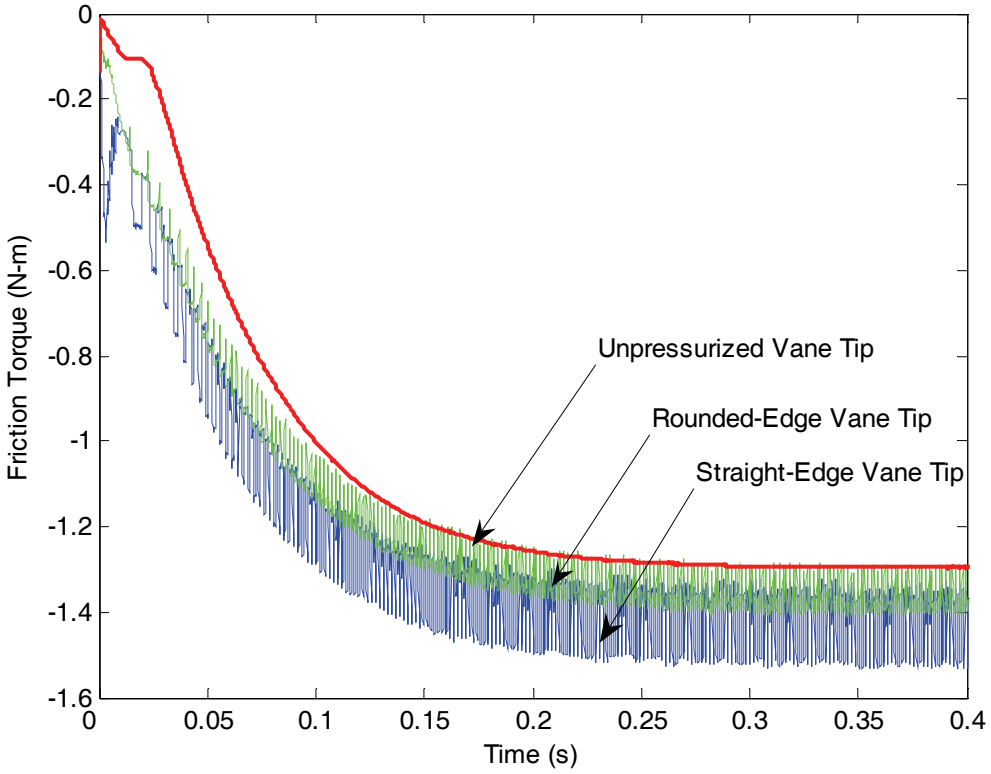

Figure 25. Comparison plots of total friction torque.

The total friction in the system is the sum of the friction torques of the six vanes. As is expected the pressurized cases have higher friction torques. Even though the rounded edge vane tip has a higher coefficient of friction, the straight-edge vane tip has a higher friction torque. The normal force of the straight-edge vane is higher than the rounded edge vane which causes the overall friction torque to be higher. Again, the pressurized cases tend to oscillate more due to the fact that vanes are entering and exiting pressurized areas. The unpressurized case also oscillates, but it oscillates with a much lower amplitude.

Increasing friction forces decrease the net torque in the system. Figure 26 displays the net torque of the system

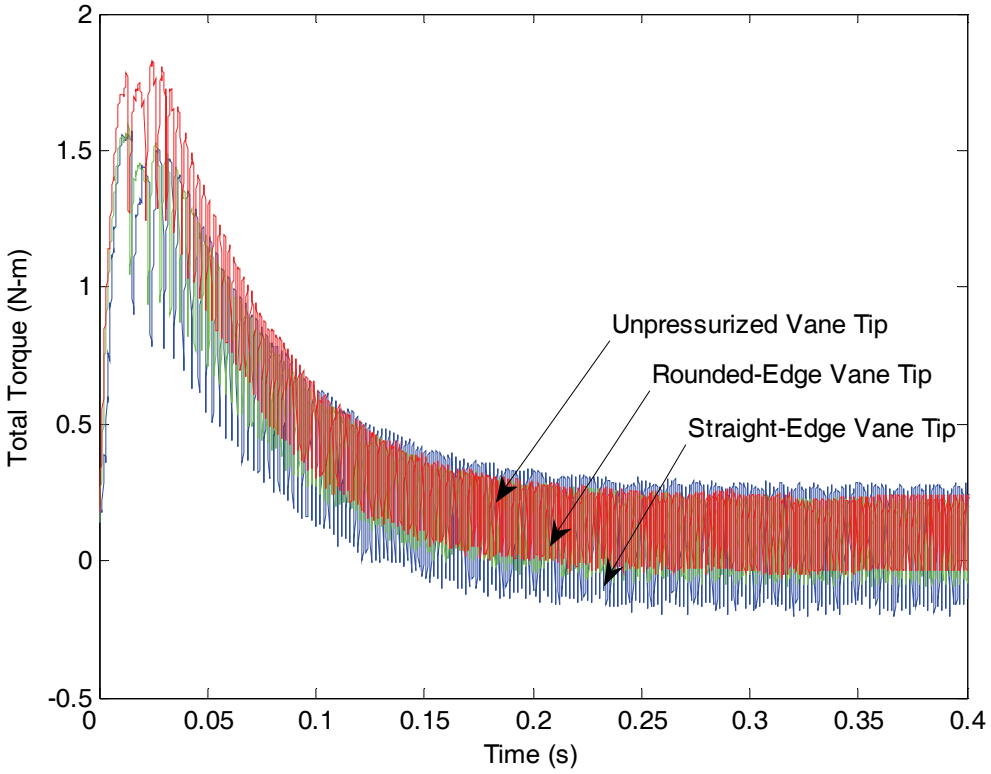

Figure 26. Comparison plot of the total torque of the system.

For all cases, the total torque should eventually decrease to zero once a steady velocity is achieved. Due to long simulation times, only enough data to reach a negligible amount of torque was taken. The total torque of the system decreases slightly faster for the pressurized cases. The straight-edge vane decreases the fastest, which means that it should give a poorer performance than a hot gas vane motor with rounded edges due to friction losses. Also, the unpressurized case tends to oscillate less than the pressurized cases since the friction torque oscillates more when the vanes are pressurized. The unpressurized case's total torque oscillated over a range of 0.2 N-m while the rounded edge and straight-edge vane cases oscillated over a range of 0.25 N-m and 0.5 N-m respectively.

Lower torques mean lower angular velocities. Figure 27 displays the angular velocities of the three cases under discussion.

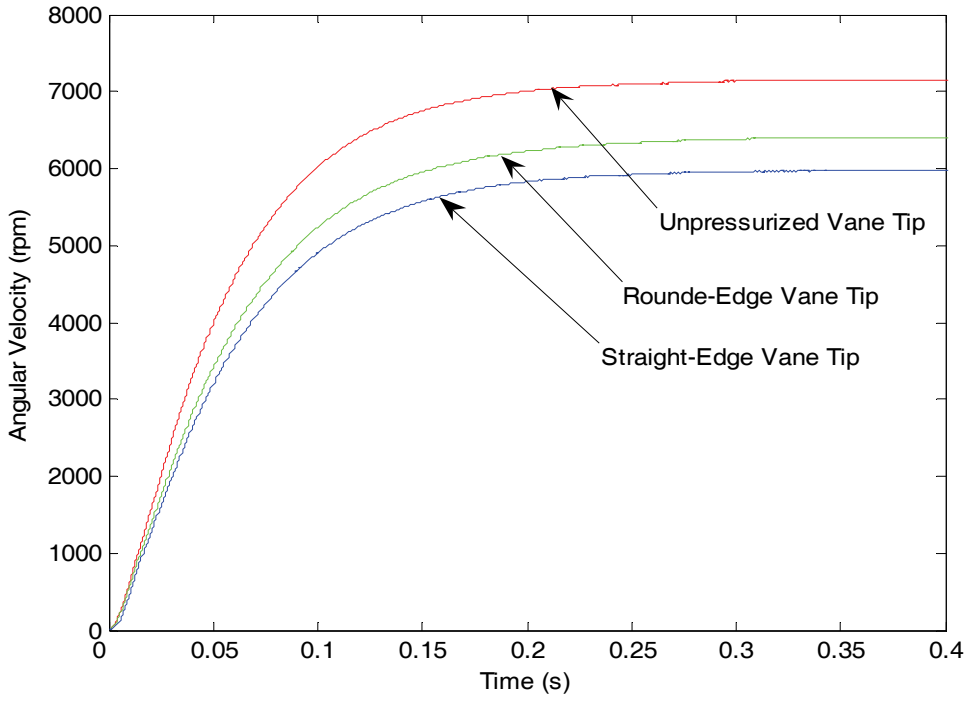

Figure 27. Comparison plot of angular velocities.

As is expected the unpressurized vane tip case experiences the highest angular velocity, 7,100 rpm. The pressurized cases rotate slightly slower, 6,400 rpm and 6,000 rpm for the rounded edge and straight-edge vane tip respectively. The lower angular velocities are due to the added pressure forces, which create friction

The unpressurized case is an unreasonable situation. Pressure needs to be included in the design, because without pressure forces on the vane, the chambers of the hot gas vane motor could not remain sealed. If the chambers are not sealed, then massive amounts of leakage will occur within the device causing very poor performance. To ensure that a minimal amount of leakage occurs between chambers, the backside of each vane needs to be pressurized to counteract the pressure forces on the tip. To minimize the amount of friction losses a rounded edge vane tip should be used.

Chapter 5

Efficiency Modeling

5.1 Discussion of Efficiency

The first objective of this work was to model and understand the operation of a vane motor. Then the developed model could be used to optimize the performance of the device. The efficiency of a vane motor is based primarily on the geometry of the device. By properly designing the dimensions of the stator and rotor relative to each other, it is anticipated that better performance and efficiency can be observed.

In order to optimize the performance of the hot gas vane motor, a measure of performance must first be defined. For this work, the efficiency is a comparison of the amount of energy that is injected into the motor compared to the amount of energy that is wasted by means of exhausting hot gas from the system. The highest possible efficiency of the motor is defined by the following from [1]:

$$\eta = 1 - \left(\frac{V_1}{V_2}\right)^{\gamma-1} = \frac{P_1V_1 - P_2V_2}{P_1V_1} = \frac{Useful\ Energy}{Energy\ in} \tag{5.1}$$

where $\frac{V_1}{V_2}$ is the expansion ratio of the volumes, P_1 is the initial pressure, P_2 is the pressure prior to exhaust, and γ is a ratio of specific heats. The initial volume, V_1, is the smallest volume of a full chamber at the beginning of the cycle which for the model occurs at 90 degrees and is approximately 1.215e-6 m^3. At 90 degrees, a chamber is cut off from the injection port so the chamber is full of hot gas and is at its smallest volume. The final volume, V_2, is the largest volume a chamber reaches just prior to the exhaust phase of the cycle which occurs at 210 degrees and is

approximately 3.11e-6 m^3. From Eqn. (5.1), it can be shown that with the current geometry the highest possible efficiency of the vane motor is approximately 27.7%. This efficiency does not take into account heat loss, leakage, or friction effects. Also, it is assumed that throughout the operation of the device, the propellant remains a gas, which is not necessarily the case. The expansion ratio of the hot gas during operation determines how much torque can be created by the device. To optimize the vane motor, different motor geometries should be tested to see if any major changes in performance or efficiency are observed.

The total efficiency of any system is just a ratio of the energy supplied to the system and the amount of energy that is produced as usable work. The internal energy entering the system is defined by the following,

$$E_1 = \frac{P_1 V_1}{\gamma - 1} \tag{5.2}$$

where P_1 is the pressure at the inlet and V_1 is the inlet volume. Ideally the total internal energy from a single chamber is 3.86 Nm. The amount of energy that is wasted through exhaust by the system is defined by the following,

$$E_2 = \frac{P_2 V_2}{\gamma - 1} \tag{5.3}$$

where P_2 is the pressure in the chamber just prior to exhaust and V_2 is the volume in the chamber just prior to exhaust. Equation (5.3) refers to the amount of energy that is wasted by exhausting the hot gas. The pressure in the chambers at "steady" speed operation may be viewed in Figure 28.

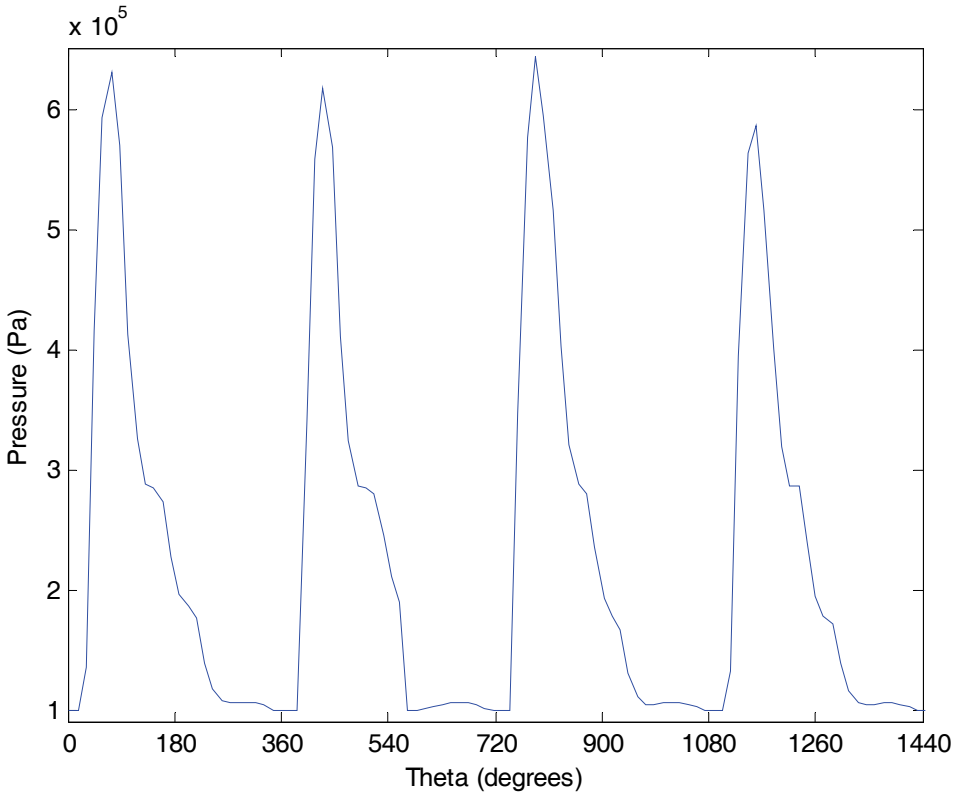

Figure 28. Pressure in a single chamber.

The pressure in the chamber just prior to exhaust is about 310,000 Pa. This means that the amount of energy that is wasted through exhaust is 2.8 Nm.

The ideal efficiency from Eqn. (5.1) uses the assumption that E_1 and E_2 are the only energies present within the system. For a more accurate description of the efficiency of the vane motor, the energy dissipated due to friction was considered. The actual efficiency of the vane motor is defined by the following,

$$\eta = \frac{n(E_1 - E_2) - W_f}{nE_1} \tag{5.4}$$

where n is the number of chambers, and W_f is the energy dissipated due to friction. The total amount of energy that is wasted as a result of friction may be determined from dynamics by integrating the frictional force, F_f, with respect to the path of the

vane using the following,

$$W_f = \int_0^{2\pi} F_f(\theta) \bullet dr \tag{5.5}$$

Since the force is always parallel to the stator surface, *dr* is simply an arc on the stator which may be defined as $ld\theta$ where *l* is the distance from the center of rotation on the rotor to the edge of the stator as was defined by Eqn. (3.2). The following simplified equation may be used to solve for the energy dissipated as a result of friction,

$$W_f = \int_0^{2\pi} F_f(\theta) \bullet dr \simeq \int_0^{2\pi} F_f(\theta) l(\theta) d\theta \tag{5.6}$$

The efficiency can now be solved for using Eqn. (5.4). By including the affects of friction the efficiency of the device is reduced from 27.7% to 8.8%.

5.2 Results

In order to optimize the design of the hot gas vane motor, the preceding analysis was duplicated using several different vane geometries. Vane motors can be designed in numerous sizes and shapes, and it is desirable to know how the size of the motor will affect its performance. The following figure displays how both the ideal efficiency and the efficiency as computed by the model vary with the radius of the stator.

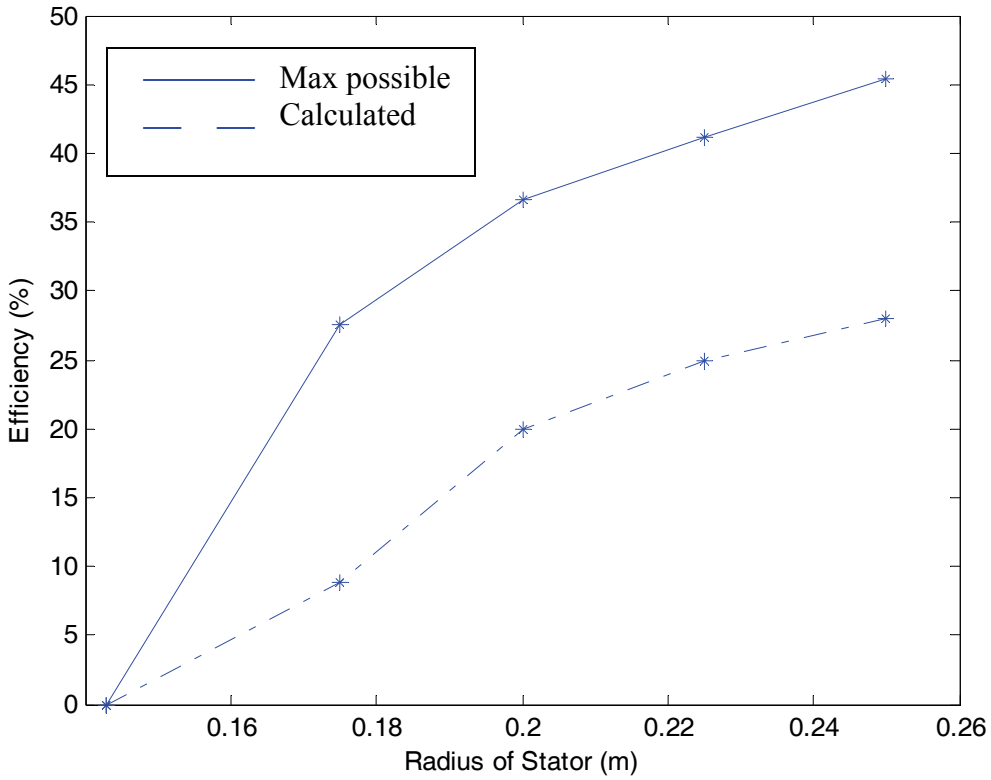

Figure 29. Actual and maximum efficiencies of vane motors with various stator radii.

Both the affects of friction and the affects of pressure were considered for the analysis. It was assumed that the ends of the vane tips were rounded. It was shown in Chapter 4 that rounded edge vane tips tend to reduce the amount of friction as compared with vanes with straight tips. The maximum efficiency increases with a larger stator radius, which is expected since increasing the stator radius increases the volume expansion ratio. The actual efficiency also increases substantially. The length of the stator radius is limited by the distance between the rotor and stator. If the distance is too great the vane will slip from the rotor which is obviously undesirable. However, designing a motor with a larger stator radius does seem to produce better

results. Increasing the stator size increases the efficiency of the device by increasing the expansion ratio of the hot gas. Increasing expansion ratio ensures that less gas is wasted through exhaust.

Chapter 6

Conclusions

6.1 Overview

The main objectives of this work were to first establish a working model of a hot gas vane motor. Then, a means for measuring performance was presented by way of efficiency. Finally, the model was used to show that by adjusting certain parameters, the overall efficiency of the device could be improved.

The model presented is based primarily on determining the net amount of torque produced by the device. The amount of torque in the system is dependant on the amount of pressure in the system. By using equations for pressure based on an isentropic process, a model of the amount of torque created may be developed. Next, it was shown that the amount of friction within the system has a significant affect on the performance of the device. It was shown in Chapter 3 that dynamic equations may be used to solve for the acceleration of the vanes in the direction normal to the stator's surface, which may be used to solve for the friction torque between the vane tips and the stator. Without friction, the simulations showed that the device would rotate at nearly 25,000 rpm and that steady state velocity could be approached in 2 seconds. When friction was included, the simulation showed that the device would rotate at a much lower speed, 7,100 rpm, and approach steady state in 0.4 seconds. The simulation with friction is a much more reasonable result for the performance of a hot gas vane motor. Typical vane motors do not exceed 13,000 rpm in angular velocity.

A comparison of the forces created from centripetal and relative acceleration to the forces created from pressures on the ends of the vanes was presented in Chapter 4. By including the pressure calculations, it was shown that the amount of friction within the system was increased due to the increase in normal force. The total torque in the system oscillated more when pressure forces were included, because the pressure forces spiked during the working phase and were negligible during the exhaust phase. The presence of pressure causes the torque to oscillate over a range of 0.25 N-m in the case of a rounded edge vane tip, and 0.5 N-m in the case of a straight-edge vane tip. With no pressure present on the ends of the vanes, the total torque oscillated over a range of only 0.2 N-m. The angular velocity of the vane motor is reduced from 7,100 rpm to 6,300 rpm in the case of a rounded edge vane tip or to 6,000 rpm in the case of a straight-edge vane tip. A rounded edge vane tip reduces the amount of friction in the system by reducing the affects of pressure on contact forces between vane and rotor.

Finally, it was shown that the geometry of the device may be adjusted to improve the efficiency of the motor. Hot gas vane motors with larger expansion ratios have higher efficiencies than motors with low expansion ratios. The expansion ratio may be increased by increasing the size of the stator relative to the rotor. With a larger expansion ratio, less usable work is wasted through exhausting gas.

6.2 Future Work/Recommendations

Future plans for this work are to improve on the existing model. The current model accounts for the friction at the tip of the vane, but friction on the side of the

vanes was not considered. Research has shown that the majority of friction is present on the vane tips, but friction is present on the side as well [6]. This friction needs to be accounted for in order to improve the accuracy of the model.

Also, in order to improve the accuracy of the model, other losses besides friction need to be considered. In any pneumatic or hydraulic device leakage will occur. In the case of a hot gas vane motor, leakage is most likely present between pressurized chambers. Leakage of the hot gases would cause the pressure in working chambers to decrease which would cause the net torque to decrease causing the efficiency and performance of the device to decrease as well. Other losses that may need to be considered would be losses from heat loss. The hot gas vane motor operates at a high temperature and is dependant on the hot gas remaining a gas throughout operation. If any gas condensed to a liquid, then the pressure in the chambers would be reduced causing a decrease in efficiency.

Other future work includes varying more parameters to see how efficiency is affected. The width of the vane would not change the maximum efficiency of the device since the expansion ratio remains constant, but the actual efficiency may be altered due to increases in friction. Also, varying the injection pressure on the device could alter the performance so inlet pressure should be varied to study the affects. For this work no load torque was included on the device, so a study of the affects of adding load torque could be added.

The best way to check the accuracy of the model created, would be to test it against actual experimental data. Future plans of this work are to design and test an actual vane motor, and check the modeled results against the experimental data. Then

the updated model may be used to optimize the efficiency of the device. The main component of this research that is still needed is experimental results to support the simulation results.

References

[1] E. Barth, K. Fite, M. Goldfarb, B. Li, "Design of a Hot Gas Vane Motor," IMECE, November, 2004.

[2] Fluid Motors, Vane Motors, January, 2007, www.machinedesign.com.

[3] E. Wernimont, M. Ventura, G. Garboden, P. Mullens, "Past and Present Uses of Rocket Grade Hydrogen Peroxide," H202 Conference 1999.

[4] N. D. Manring, *Torque on the cylinder block of an axial-piston swash-plate type hydrostatic pump.* Ph.D. Dissertation. Iowa State University, Ames, Iowa, 1996.

[5] A. Manuello Bertetto, L. Mazza, S. Pastorelli, T. Raparelli , "A Model of Contact Forces in Pneumatic Motor Vanes," *Meccanica* Vol. 36, pp. 691-700, 2001.

[6] Y. Inaguma, A. Hibi, "Vane Pump Theory for Mechanical Efficiency," *Proc. IMechE* Vol. 219, Part C: J. Mechanical Engineering Science.

[7] B. Munson, T. Okiishi, D. Young, *Fundamentals of Fluid Mechanics*, New York: John Wiley & Sons, Inc., 1994.

[8] K. Fite, M. Goldfarb, "Design and Energetic Characterization of a Proportional-Injector Monopropellant-Powered Actuator," in *IEEE/ASME Transactions on Mechatronics*, Vol. 11, no. 2, pp. 196-204, April 2006.

[9] M. Guoyuan, Y. Qisen, Y. Yongzhang, "Dynamic Behavior of a Twin-Piece Vane Machine," in *ASME Journal of Mechanical Design* Vol. 124, pp. 74-78, March 2002.

[10] D. Greenwood, *Principles of Dynamics*, Upper Saddle River, New Jersey: Prentice Hall, 1988.

[11] N. D. Manring, "Modeling of the Torque Loss Due to Vane Friction within a Hot Gas Vane Motor," Draft, University of Missouri, Columbia, July 6, 2007.